UNIFIED APPROACH FOR THE EARLY UNDERSTANDING OF IMAGES

by

Dong-seok Jeong

Thesis submitted to the Faculty of the

Virginia Polytechnic Institute and State University

in partial fulfillment of the requirements for the degree of

Master of Science

in

Electrical Engineering

APPROVED:

Paul M. Lapsa, Chairman

A. A. (Louis) Beex

R. V. Foutz

May 1985

Blacksburg, Virginia

UNIFIED APPROACH FOR THE EARLY UNDERSTANDING OF IMAGES

by

Dong-seok Jeong

Paul M. Lapsa, Chairman

Electrical Engineering

(ABSTRACT)

In the quest for computer vision, that is the automatic understanding of images, a powerful strategy has been to model the image parametrically. Two prominent kinds of approaches have been those based on polynomial models and those based on random-field models. This thesis combines these two methodologies, deciding on the proper model by means of a general decision criterion. The unified approach also admits composite polynomial/random-field models and is applicable to other statistical models as well. This new approach has advantages in many applications, such as image identification and image segmentation. In segmentation, we achieve speed by avoiding iterative pixel-by-pixel calculations. With the general decision criterion as a sophisticated tool, we can deal with images according to a variety of model hypotheses. Our experiments with synthesized images and real images, such as Brodatz textures, illustrate some identification and segmentation uses of the unified approach.

ACKNOWLEDGEMENTS

First I would like to thank Dr. Paul M. Lapsa for his guidance and support from the beginning to final completion of this thesis. Without his guidance and support, this thesis would not have been possible. I also give thanks to Dr. A.A. Beex and Dr. R.V. Foutz who gave many valuable suggestions. I thank my parents for getting me off to a good start. Special thanks to the people who work and research in the Spatial Data Analysis Laboratory for their valuable support. I thank the Lord for giving me the strength to persevere. To my beautiful daughter I love you and thank you for tolerating your student Dad. Finally, no amount of words can express the love and appreciation I feel for my loving wife , who supported me all the way.

TABLE OF CONTENTS

CHAPTER 1. INTRODUCTION

1.1) MOTIVATION

Ideally, the computer vision problem, that is, the algorithmic understanding of images, could be thought of as a problem in testing statistical hypotheses. However, in most applications, the immediate use of even the simplest statistical approach runs into great computational difficulties.

Also we understand the fact that it is impossible to build a universally capable machine which can perform arbitrary classifications of multi-dimensional patterns, such as images. So the solution of the recognition problem must be based on **a priori postulates** concerning the subsets of images to be recognized out of the set of all possible images. That will narrow the collection of possible classifications. To specify concrete a priori postulates, we describe the images to be recognized by means of **parametric models**, i.e. we define the stochastic dependence among image pixels by means of various parameters.

The recognition problem can then be seen as that of adopting an optimal decision as to the nature and values of parameters. The parametric model concept allows us to adopt a single point of view with regard to various recognition methods and various formulations of the problems.

The criterion of optimality can be based on the probability of making a wrong decision, or the a posteriori probability, or the likelihood. The likelihood is usually the easiest quantity to describe and compute. Also we know that under certain conditions the maximization of the likelihood function is equivalent to minimizing the probability of making a wrong decision. This is usually the goal of pattern recognition in practical applications.

Broadly speaking, two prominent, distinct classes of research approaches to the problem of representing images are those based on **polynomial facet models** and those based on **random-field models**. In polynomial facet model approaches, the image to be understood is modeled (hypothesized) as the polynomials, and the parameters are estimated by one of many established techniques such as maximum likelihood. Then using some decision criterion, which is valid only for this model hypothesis, the image is classified into one of a number of pre-defined categories. The same arguments are applied for the random-field model approaches, i.e. parameter estimation, decision criterion, and classification.

Random-field models have been studied extensively and have been proved to have many applications in image processing and analysis. But from the textural point of view, buildings, roads, and shaded surfaces etc. are more adequately represented as polynomial models rather than random-field models. On the other hand, visual textures such as trees (with leaves), grasses, and sand are more likely to be hypothesized as random-field models rather than polynomial models. So those two approaches have compensating advantages and limitations. Also it is not difficult to expect that those methods are each subject to various constraints and assumptions which limit their performance.

Therefore it is more realistic to assume that a certain context (i.e. a subject image) has both random-field parts and polynomial parts rather than only one of them. We can easily expect that **if we can combine both techniques in some way, the perfomance will be improved** in the sense of effectiveness and correctness of representation. But so far most researches have pursued separate approaches without attempting to unify them into a universally encompassing technique. Probably the main obstacle of combining them is the lack of a convenient, effective **general decision strategy** which can distinguish among polynomial model hypotheses, random-field model hypotheses, or combination of these.

We derive such a general decision criterion in detail, and refer to this new method as a **unified approach**. This method combines both approaches mentioned above, in that it can handle a variety of model hypotheses such as pure polynomial facet models, pure random-field models, or composites thereof. In addition to the versatility of handling many kinds of visual textures, this proposed approach has strong advantages in segmenting the images. Unlike most other segmenting schemes which rely heavily on iterative calculations, our method minimizes iteration, which implies a dramatic reduction of computations and improvement of speed. Also the result of our segmentation is not only a pixel-labeled image, but also an explicit list of regions; so the result is in a form which is a convenient input for higher-level processing such as artificial-intelligence approaches to computer vision.

1.2) LITERATURE REVIEW

The following review of literature is not exhaustive: we will mention only those papers which are closely related to our topics. The first section will deal with the **synthesis** of the images. Because the synthesis of polynomial image is rather straightforward, we only concentrate on the synthesis of random-field images. The second section will review the literature dealing with **image analysis** such as parameter estimation and image identification. The third part will survey the literature dealing with **image segmentation** techniques from the standpoint of the assumption that an image should satisfy some "models" in order for a particular technique to be applicable to it.

Synthetic Generation of Random Field Images

A Random Field can simply be defined as a random process evolving in more than one dimension [1]. One of the early observations of this concept was made by Whittle in 1954 [2]. Whittle's paper outlines the basic approach for a stationary, autoregressive, scalar random field by extending spectral methods he developed for time series. However, this was before the high-speed computer and fast Fourier transforms became popular, so that these spectral methods anticipated the convenient computations of the later decades. Of the numerous papers that have been published after Whittle's paper, deserving special attention is Larimore's tutorial paper [3] on statistical inference on stationary random fields. He discusses algorithms for fitting parametric models and testing hypotheses between alternative model structures. Besag [17] examines several stochastic models which may be used to describe spatial processes. He distinguishes between the conditional probability approach to spatial interaction and the alternative joint probability approach, in that the former is more general than the latter.

Synthetic Generation of images obeying known SAR[1] and CM[2] models were actively studied by Kashyap, Chellapa, and Lapsa [1,4,5,6]. The synthetic generation of even a small random-field image can involve difficult computations in principle, but by means of fast Fourier transform algorithms, we can easily synthesize the images of various models. For example, recently algorithms for synthesizing 2-D NCAR[3] models were discussed by Chellapa and Kashyap [7].

---

1 Simultaneous AutoRegressive

2 Conditional Markov

3 Non-Causal AutoRegressive

Image Analysis

Parameter Estimates in general can be obtained by the maximum likelihood (ML) method [3], but the ML scheme can lead to nonlinear optimization problems. There are ways to avoid excessive calculation; for example, Kashyap and Chellapa proposed an approximate scheme for SAR models [6]. They also discussed advantages over the computationally simpler MS[4] estimates, which are not consistent for non-unilateral models.

Image Identification can be defined as choosing the proper model structure to characterize a given image, i.e. identifying the image as belonging to a certain parameterization [8]. Some criteria used for image identification are explained in [3,8,9,10]. As a recent application, Bolle and Cooper [18] try to recognize 3-D shapes by approximating the observed pixel intensities with quadratic polynomials.

Segmentation

Probably one of the most active research areas in image processing is segmentation, which can be thought of as the division of images into regions obeying different models. Thus for an image that does not obey a single model in its entirety, a logical step is to try to segment it so that each partition does obey a certain model.

---

[4] Mean Square

Broadly speaking, there are two ways of segmenting an image: by delineating the boundaries surrounding its regions, or by extracting its homogeneous areas directly [11]. The latter approach has important theoretical advantages, but is subject to greater computational difficulties. Our method provides an algorithm for implementing it effectively.

A tutorial paper by Rosenfeld and Davis [11] describes various approaches to segmentation. Also Fu and Mui [12] published a tutorial paper about segmentation in which three prevalent methods, i.e. threshold and clustering, edge detection, and region extraction, are explained. Rosenfeld updated his survey on segmentation techniques in 1984. [21]

Because most images of natural scenes can be effectively characterized as composites of textures, segmentation by texture is especially interesting. Therrien [13] applied ML and MAP algorithms to estimate regions of similar terrain and used this technique to segment aerial photographic data. Kashyap and Lapsa [8] proposed a segmentation scheme which uses a decision criterion as a tool. They applied this scheme to the images composed of two regions of different random fields. Bevington and Mersereau [14] also discussed the problem of segmenting an image by texture. Specifically they are concerned with estimating the edge between regions characterized by different two-dimensional autocorrelation functions. Also papers by Horowitz and Pavlidis [15], and Chen and Pavlidis [16] deserve to be mentioned. They used estimation approaches to segmentation and tried a split-and-merge concept for defining regions.

1.3) ORGANIZATION OF MATERIAL

The remainder of this thesis is organized as follows. In chapter 2, we review a standard decision theory and develop ML estimates for the given contexts. Then in chapter 3, we derive the general decision criterion which can be used on any kind of hypothesis. The decision criterion then is applied to simultaneous autoregressive models in chapter 4. A brief definition and a synthesis of an autoregressive image is also given in chapter 4. Chapter 5 is devoted to polynomial regressive images. In chapter 6, our decision criterion is applied to composite autoregressive-polynomial models. In chapter 3 through chapter 6, we give several examples of these models. Various experiments and their results are described in chapter 7. These include synthesis, estimation, identification, and segmentation. Finally some limitations and constraints of our scheme are discussed in chapter 8, and some extensions of the presented method are suggested.

CHAPTER 2. STANDARD DECISION THEORY

2.1) STANDARD DECISION THEORY

The notation and standard theory as in [8] will be used, and it is repeated in this section for convenience. Let the models under consideration, r in number, be denoted by

$$H_1, H_2, \quad \ldots \quad , H_r$$

The data

$$y_s \varepsilon R^{M^2} \qquad (2.1)$$

where

$M^2 = m$ = number of samples,

are presumed to have arisen from one of the models.

Let the a priori probability that the k-th model generated the data be $P(H_k)$. For example, in the absence of other knowledge, the typical assumption is that

$$P(H_k) = \frac{1}{r}, \qquad k=1,2, \quad \ldots \quad ,r \qquad (2.2)$$

Also let $f_k(\alpha_k)$ be the a priori density of the model's n_k parameters contained in the vector

$$\alpha_k \ \varepsilon \ \Omega_k \subseteq R^{n_k}$$

$$(k = 1,2, \quad \dots \quad ,r)$$

A decision rule for selecting a model based on the observations associates one of H_1, H_2, - - - , H_r with each possible data point in expression (2.1).

In other words, the decision rule partitions the observation space in (2.1) into the regions D_1, D_2, - - - , D_r so that the data in D_j is assigned to model H_j.

If the true hypothesis is H_k, then this decision rule incurs a probability of error Q_k given by

$$Q_k = \sum_{j=1}^{r} \int_{D_j} dy_s \int_{\Omega_k} d\alpha_k \, p_k(y_s;\alpha_k) \, f(\alpha_k) \quad , \ j \neq k \tag{2.3}$$

The average probability of error is

$$E = \sum_{k=1}^{r} P(H_k) \, Q_k \tag{2.4}$$

The decision rule which minimizes E is that corresponding to the optimal partition $D_1^*, D_2^*, \ldots, D_r^*$ defined by

$$D_i^* = \{y_s : p(H_i|y_s) \geq p(H_j|y_s), \text{ for all } j \neq i\} \tag{2.5}$$

where the $P(H_k|y_s)$ are the a posteriori probabilities of the models.

In short, given the data y_s, we choose the hypothesis H_i which gives the largest $P(H_i|y_s)$.

It remains then to evaluate these probabilities. By Bayes' rule,

$$p(H_k|y_s) = \frac{p(y_s|H_k)\ P(H_k)}{\sum_j p(y_s|H_j)\ P(H_j)} = C\ p(y_s|H_k)\ P(H_k) \tag{2.6}$$

where

$$p(y_s|H_k) = \int_\Omega d\alpha_k\ p_k(y_s;\alpha_k)\ f(\alpha_k)$$

and C is a constant independent of H_k.

2.2) APPROXIMATION IN TERMS OF MLE.

We now discuss $P(y_s|H_k)$ in more detail [22]. Again,

$$p(y_s|H_k) = \int_{\Omega_k} d\alpha_k\ p_k(y_s;\alpha_k)\ f(\alpha_k) \tag{2.7}$$

To get the $p(y_s|H_k)$, we need to derive $p_k(y_s;\alpha_k)$, where y_s represents all the samples. We assume suitable regularity conditions and approximate $p_k(y_s;\alpha_k)$ in terms of its value at the maximum likelihood estimate α_k^*. The Taylor series for a function of one variable is

$$f(x) = f(a) + f'(a)\ (x-a) + \frac{f''(a)\ (x-a)^2}{2!} + \text{h.o.t.} \tag{2.8}$$

Let $f(x)$ be $\ln p_k(y_s;\alpha_k)$, and $f(a)$ be $\ln p_k(y_s;\alpha_k^*)$, where α_k^* is the maximum likelihood estimate (MLE) of α_k. Then, $(x-a)$ is associated with $(\alpha_k - \alpha_k^*)$. Rewriting (2.8) with the above parameters,

$$\ln p_k(y_s;\alpha_k) = \ln p_k(y_s;\alpha_k^*) + (\alpha_k-\alpha_k^*)^T\ \nabla_{\alpha_k}[\ln p_k(y_s;\alpha_k^*)]$$

$$+ \frac{1}{2}\ (\alpha_k-\alpha_k^*)^T\ \nabla^2_{\alpha_k\alpha_k}[\ln p_k(y_s;\alpha_k^*)]\ (\alpha_k-\alpha_k^*) + \text{h.o.t.} \tag{2.9}$$

Because α_k^* is the MLE,

$$\nabla_{\alpha_k}[\ \ln p_k(y_s;\alpha_k)\ ] = \underline{0} \quad \text{at} \quad \alpha_k = \alpha_k^* \tag{2.10}$$

So,

$$\nabla_{\alpha_k}[\ \ln p_k(y_s;\alpha_k^*)\ ] = \underline{0} \tag{2.11}$$

Let

$$I_m(\alpha_k^*) \equiv \frac{-1}{m} \nabla^2_{\alpha_k \alpha_k} [\ \ln p_k(y_s;\alpha_k^*) \ ] \tag{2.12}$$

where m is the number of samples. With (2.11) and (2.12), equation (2.9) becomes

$$\ln p_k(y_s;\alpha_k) = \ln p_k(y_s;\alpha_k^*)$$

$$+ \frac{-1}{2} (\alpha_k - \alpha_k^*)^T [m \ I_m(\alpha_k^*)] \ (\alpha_k - \alpha_k^*) + \text{h.o.t.} \tag{2.13}$$

Thus

$$p_k(y_s;\alpha_k) \simeq p_k(y_s;\alpha_k^*) \quad \exp\{ \frac{-1}{2} (\alpha_k - \alpha_k^*)^T [m \ I_m(\alpha_k^*)] \ (\alpha_k - \alpha_k^*)\} \tag{2.14}$$

For large m, i.e. with enough samples,

$$\alpha_k^* \simeq \alpha_k$$

Then

$$I_m(\alpha_k^*) \simeq I(\alpha_k) = E\{ \ - \nabla^2_{\alpha_k \alpha_k} \ln p_k((y_s);\alpha_k) \ \} \tag{2.15}$$

where (y_s) denotes a single sample of m independent and identically distributed samples. $I(\alpha_k)$, the Fisher information matrix, is not a function of m.

Therefore, for m large, the expression for $p_k(y_s;\bar{\alpha}_k)$ is, except for a normalizing constant, a Gaussian function with variable α_k, and from (2.14) and (2.15) the covariance matrix is

$$\Sigma_m = [\, m \ I_m(\alpha_k^*) \,]^{-1}$$
$$= \frac{1}{m} [\, I_m(\alpha_k^*) \,]^{-1} \simeq \frac{1}{m} [\, I\,(\alpha_k) \,]^{-1} \tag{2.16}$$

Thus, (2.16) becomes arbitrarily small as m gets large.

Now let us rewrite the equation (2.7),

$$p(y_s|H_k) = \int_{\Omega_k} d\alpha_k \ p_k(y_s;\alpha_k) \ f(\alpha_k)$$

$$= \int_{\Omega_k} p_k(y_s;\alpha_k^*) \exp\{ \frac{-1}{2} (\alpha_k-\alpha_k^*)^T [m \ I_m(\alpha_k^*)] \ (\alpha_k-\alpha_k^*) \ \} \ f(\alpha_k) \ d\alpha_k$$

$$= p_k(y_s;\alpha_k^*) \ \int_{\Omega_k} \exp\{ \frac{-1}{2} (\alpha_k-\alpha_k^*)^T [m \ I_m(\alpha_k^*)] \ (\alpha_k-\alpha_k^*) \ \} \ f(\alpha_k) \ d\alpha_k \tag{2.17}$$

Because of the large-sample behavior of Σ_m in (2.16), the support for the integration over Ω_k is essentially near α_k^*. With m large,

$$\alpha_k^* \simeq \alpha_k$$

Therefore,

$$f(\alpha_k) \simeq f(\alpha_k^*)$$

So (2.17) becomes

$$p(y_s|H_k) \simeq p_k(y_s;\alpha_k^*)\ f(\alpha_k^*) \int_{\Omega_k} \exp\{-\frac{1}{2}(\alpha_k-\alpha_k^*)^T [m\ I_m(\alpha_k^*)](\alpha_k-\alpha_k^*)\}d\alpha_k \quad (2.18)$$

Recalling the formula for the area under the Gaussian curve,

$$\int_{\Omega_k} \exp\{ -\frac{1}{2}(\alpha_k- \alpha_k^*)^T [m\ I_m(\alpha_k^*)]\ (\alpha_k- \alpha_k^*)\ \}\ d\alpha_k$$

$$= (2\pi)^{n_k/2} \det^{-1/2} [m\ I_m(\alpha_k^*)] \quad (2.19)$$

where n_k is the dimension of α_k, i.e. the number of parameters. With (2.19), (2.18) becomes

$$p(y_s|H_k) \simeq p_k(y_s;\alpha_k^*)\ f(\alpha_k^*)\ (2\pi)^{n_k/2} \det^{-1/2} [m\ I_m(\alpha_k^*)] \quad (2.20)$$

Simplifying,

$$p(y_s|H_k) \simeq p_k(y_s;\alpha_k^*)\ f(\alpha_k^*)\ (2\pi)^{n_k/2} \det^{-1/2} [I_m(\alpha_k^*)]\ \ m^{-n_k/2} \quad (2.21)$$

Then finally

$$\ln p(y_s|H_k) \simeq \ln p_k(y_s;\alpha_k^*) + \frac{-n_k}{2} \ln \frac{m}{2\pi} + \frac{-1}{2} \ln \det[I_m(\alpha_k^*)] + \ln f(\alpha_k^*) \tag{2.22}$$

So, $p(y_s|H_k)$ is approximated in terms of the estimated parameter vector α_k^*.

CHAPTER 3. GENERAL DECISION CRITERION

With the knowledge of chapter 2, let us proceed to derive the general decision criterion. Rewriting Eq.(2.6) with logarithm

$$\ln p(H_k|y_s) = \ln C + \ln p(y_s|H_k) + \ln P(H_k) \tag{3.23}$$

Also recalling Eq.(2.5), the optimum decision for sample y_s is made when we choose the hypothesis H_i which gives the largest $p(H_i|y_s)$.

So if assumption (2.2) is used, the value of $\ln p(H_k|y_s)$ depends only on the value of $\ln p(y_s|H_k)$.[5] We already derived the approximation of $\ln p(y_s|H_k)$ at Eq.(2.22). Rewriting it,

$$\ln p(y_s|H_k) \approx \ln p_k(y_s;\alpha_k^*) + \frac{-n_k}{2} \ln \frac{m}{2\pi} + \frac{-1}{2} \ln \det[\, I_m(\alpha_k^*)\,] + \ln f(\alpha_k^*) \tag{3.24}$$

So Eq.(3.24) is the actual formula which gives the decision criterion. The next step is to develop Eq.(3.24) further by imposing a particular

[5] Modification of the decision criterion when this assumption is not used is mentioned in chapter 7.

structure on the hypothesis $p_k(y_s;\alpha_k)$. Thus, all models considered in this thesis are assumed to have the form

$$p(y_s;\alpha) = (2\pi\rho)^{-m/2} (\det{}^{-1}B)^{-1} \exp\{ \frac{-1}{2\rho} \sum_t [w_t(y_s;\phi,t)]^2 \} \tag{3.25}$$

where B is the transformation matrix from y_s to w_t (subscripts t and s refer to the sample points), and

$$\alpha = \begin{bmatrix} \phi \\ - \\ \rho \end{bmatrix}$$

Therefore

$$\ln p(y_s;\alpha) = \frac{-m}{2} \ln 2\pi\rho + \ln \det B + \frac{-1}{2\rho} \sum_{t=1}^{m} (w_t(y_s;\phi,t))^2 \tag{3.26}$$

$$\nabla_\alpha \ln p(y_s;\alpha) = \begin{bmatrix} \nabla_\phi (\ln p(y_s;\alpha)) \\ \\ \nabla_\rho (\ln p(y_s;\alpha)) \end{bmatrix} \tag{3.27}$$

$$= \begin{bmatrix} \nabla_\phi \ln \det B + \frac{-1}{\rho} \sum_t w_t \nabla_\phi w_t \\ \frac{-m}{2\rho} + \frac{1}{2\rho^2} \sum_t w_t^2 \end{bmatrix} \tag{3.28}$$

By definition, at the maximum likelihood estimate α^*,

$$\nabla_\alpha \ln p(\,y_s;\alpha)\Big|_{\alpha=\alpha^*} = \underline{0} \tag{3.29}$$

Then by (3.28) and (3.29), we get

$$\rho^* = \frac{1}{m} \sum_{t=1}^{m} (w_t(y_s;\ \phi^*,t))^2,$$

$$\frac{1}{\rho^*} \sum_t w_t\ \nabla_\phi w_t = \nabla_\phi \ln \det B(\phi^*) \tag{3.30}$$

To simplify further, let us assume ln det B = 0. This assumption is reasonable if the model represents a stable random field, and the generated image is of reasonable size. The assumption is most easily explained by following a simple one dimensional example.

[Ex.]

Let $y_t = \alpha_1 y_{(t-1)\bmod m} + w_t$;

Then $y_t - \alpha_1 y_{t-1} = w_t$.

So,

$$\begin{bmatrix} 1 & 0 & 0 & \cdots & -\alpha_1 \\ -\alpha_1 & 1 & 0 & & 0 \\ 0 & -\alpha_1 & 1 & & 0 \\ \vdots & & & \ddots & \\ \vdots & & & & \\ 0 & 0 & \cdots & -\alpha_1 & 1 \end{bmatrix} \begin{bmatrix} y_1 \\ y_2 \\ \vdots \\ y_m \end{bmatrix} = \begin{bmatrix} w_1 \\ w_2 \\ \vdots \\ w_m \end{bmatrix}$$

In matrix form,

$$B\,\underline{y} = \underline{w}\ ,$$

where B is a circulant matrix.

Because $\alpha_1 < 1$, det B ≈ 1 for m large.

So ln det B ≈ 0.

If we adopt the approximation ln det B ≈ 0, (3.26) simplifies to

$$\ln p(y_s;\alpha) \approx \frac{-m}{2} \ln 2\pi\rho + \frac{-1}{2\rho} \sum_{t=1}^{m} (w_t)^2 \tag{3.31}$$

So approximately,

$$\nabla_\alpha \ln p(y_s;\alpha) = \begin{bmatrix} \dfrac{-1}{\rho} \displaystyle\sum_{t=1}^{m} w_t \nabla_\phi w_t \\ \dfrac{-m}{2\rho} + \dfrac{1}{2\rho^2} \displaystyle\sum_{t=1}^{m} w_t^2 \end{bmatrix} \tag{3.32}$$

Again,

$$\nabla_\alpha \ln p(y_s;\alpha) \Big|_{\alpha=\alpha^*} = \underline{0} \tag{3.33}$$

So by (3.32) and (3.33), we get

$$\sum_{t=1}^{m} w_t \nabla_\phi w_t = \underline{0} \tag{3.34}$$

$$\rho^* = \frac{1}{m} \sum_{t=1}^{m} w_t^{\,2} \tag{3.35}$$

Now we proceed to derive $I_m(\alpha)$. Rewriting (2.12),

$$I_m(\alpha) = \frac{-1}{m} \nabla^2_{\alpha\alpha} [\ln p(y_s;\alpha)] \tag{3.36}$$

Using (3.32)

$$\frac{-1}{m} \nabla^2_{\alpha\alpha} [\ln p(y_s;\alpha)] = \frac{-1}{m} \nabla_\alpha \begin{bmatrix} \frac{-1}{\rho} \sum_{t=1}^{m} w_t \nabla_\phi w_t \\ \frac{-m}{2\rho} + \frac{1}{2\rho^2} \sum_{t=1}^{m} w_t^{\,2} \end{bmatrix} \tag{3.37}$$

Developing above differentiation and applying the relations in (3.34) and (3.35), we get the following expression

$$I_m(\alpha^*) = \begin{bmatrix} \frac{1}{m\rho^*} \sum_{t=1}^{m} [\nabla_\phi w_t] [\nabla_\phi w_t]^T & 0 \\ 0 & (2\rho^{*2})^{-1} \end{bmatrix} \tag{3.38}$$

with the relation

$$\nabla^2_{\phi\phi} w_t = 0 \tag{3.39}$$

Eq.(3.39) is valid if w_t is a linear function of the parameters, e.g. of the form

$$
\begin{aligned}
w_t &= y_t - \theta_0 - \theta_1 y_{t-1} - \theta_2 y_{t-2} \cdots - \theta_k y_{t-k} \\
&= y_t - \theta_0 - \sum_{i=1}^{k} \theta_i y_{t-i}
\end{aligned}
\tag{3.40}
$$

In that case,

$$
\nabla_\phi w_t = \begin{bmatrix} -1 \\ y_{t-1} \\ \cdot \\ \cdot \\ y_{t-k} \end{bmatrix}
$$

So, $\nabla^2_{\phi\phi} w_t = \underline{0}$

where $\phi = [\ \theta_0 \ \ \theta_1 \ \ \ldots \ \ \theta_k\ ]^T$

After some manipulations using (3.31) and (3.38), finally $\ln p(y_s|H_k)$ can be described as below.

$$
\begin{aligned}
\ln p(y_s|H_k) \simeq\ & \ln p_k(y_s;\alpha_k^*) + \frac{-n_k}{2} \ln \frac{m}{2\pi} \\
& + \frac{-1}{2} \ln \det[\ I_m(\alpha_k^*)\ ] + \ln f(\alpha_k^*)
\end{aligned}
\tag{3.41}
$$

$$= \frac{-m}{2} \ln 2\pi\rho^{*} + \frac{-1}{2\rho} \sum_{t=1}^{m} (w_t)^2 + \frac{-n_k}{2} \ln \frac{m}{2\pi}$$

$$+ \frac{-1}{2} \ln \frac{1}{2\rho^{*2}} + \frac{-1}{2} \ln \det[S_m(\alpha_k^{*})] + \ln f(\alpha_k^{*}) \qquad (3.42)$$

where
$$S_m(\alpha_k^{*}) = \frac{1}{m\rho^{*}} \sum_{t=1}^{m} [\nabla_\phi w_t] [\nabla_\phi w_t]^T \qquad (3.43)$$

Using the relation (3.35)

$$\frac{1}{2\rho^{*}} \sum_{t=1}^{m} w_t^{2} = \frac{m}{2} \qquad (3.44)$$

With (3.44), (3.42) becomes

$$\ln p(y_s|H_k) = \frac{-m}{2} \ln 2\pi\rho^{*} + \frac{-m}{2} + \frac{-n_k}{2} \ln \frac{m}{2\pi}$$

$$+ \frac{-1}{2} \ln \frac{1}{2\rho^{*2}} + \frac{-1}{2} \ln \det[S_m(\alpha_k^{*})] + \ln f(\alpha_k^{*}) \qquad (3.45)$$

With some of the terms combined, (3.45) results in

$$\ln p(y_s|H_k) = \frac{-m+2}{2} \ln \rho^{*} + \frac{-m}{2} (\ln 2\pi + 1) + \frac{-n_k}{2} \ln \frac{m}{2\pi}$$

$$+ \frac{1}{2} \ln 2 + \frac{-1}{2} \ln \det[S_m(\alpha_k^{*})] + \ln f(\alpha_k^{*}) \qquad (3.46)$$

So (3.46) is the expression of the decision criterion for the k^{th} model hypothesis. As we can see, the particulars of the particular hypothesis influence ρ and $S_m(\alpha_k)$. Also we should point out that Eq.(3.46) amounts to maximum likelihood modified by ($n_k \ln m/2\pi$) which is the penalty term. We discuss about the penalty for overparameterization in more detail at section 3 of chapter 5.

Noting that ρ is simply the average squared error attributable to that model, we only need to proceed to analyze $S_m(\alpha_k)$. The example of the simplest model is given below. A more complicated model will be discussed in a later chapter.

[Ex.] H_{00} model

$$w_t = y_t \ , \quad n_0 = 1 \ ,$$
$$\alpha_0 = [\ \rho\ ] \ , \quad \ln \det[S_m(\alpha_k^*)] = 0 \ , \quad \nabla_\phi\, w_t = 0$$

Therefore

$$\ln p(y_s|H_{00}) = \frac{-m+2}{2} \ln \rho^* + \frac{-m}{2} (\ln 2\pi + 1) + \frac{-1}{2} \ln \frac{m}{2\pi} + \frac{1}{2} \ln 2 + \ln f(\alpha_k^*) \qquad (3.47)$$

CHAPTER 4. AUTOREGRESSIVE MODEL HYPOTHESIS

4.1) DEFINITION OF SIMULTANEOUS AUTOREGRESSIVE MODEL

An image can be represented by a finite two-dimensional array of scalar data, the pixel's brightness values specified on a coordinate grid or lattice. One of the special characteristics of such data if modeled as a random field is the statistical dependence among the gray levels within a set of neighboring coordinate location, i.e. a neighbor set.

Two classes of random field models are the SAR (Simultaneous AutoRegressive) models and CM (Conditional Markov) models. These models characterize the statistical dependency of a pixel's gray level on its neighbors by a linear weighted sum of neighbors and an additive noise, independent or correlated depending upon whether the models are of the SAR or CM type.

These two classes of models are non-equivalent, in the sense that given a SAR model an equivalent CM model can always be found (equivalent in second order properties) but the converse is not always true. However it has not been clearly demonstrated whether CM models have significantly greater capability for representing natural images. In this thesis, we are primarily interested in the SAR models of finite-lattice random fields as representations of images.

In the SAR models, the dependency of a pixel's gray level on its neighbors is based on a neighbor set N, a finite set of pairs of integers, not including (0,0). Thus, for the location (i,j), the pixel gray level y(i,j) is a linear weighted sum of the members in the set

l l

$\{ y(i+k, j+1) : (k,1) \text{ is an element of } N \}$

plus independent and identically distributed noise.

To formalize the SAR models, we define some notation based on assuming the image size to be M by M pixels. The number of samples is $m=M^2$.

$J=\{0, 1, 2, \ldots , M-1\}$ is an index set.

$s=(i,j)$, such that $i,j \varepsilon J$, is a location in a finite two dimensional lattice

$y(s)$ is the image brightness or intensity at $s(i,j)$, i.e. the greytone level at pixel $s(i,j)$.

$\Omega = \{ s(i,j), i,j \varepsilon J \}$ is the set of all locations.

$\{ y(s) : s \varepsilon \Omega \}$ is the set of all data.

$E\{ y(s) \} = a$, for all $s \varepsilon \Omega$, is the mean of $y(s)$.

$N = \{ s_k = (i_k, j_k), k=1,2, \ldots, m. \ i_k, j_k \varepsilon J\}$ is a neighbor set.

$\theta(i_k, j_k)$ or $\theta(s_k)$ is a coefficient associated with neighbor location s_k. weights

With this notation, the SAR model can be formalized as

$$y(s) - a = \sum_{(i,j)\varepsilon N} \theta_{(i,j)} \{y(s \oplus (i,j) - a\} + \sqrt{\rho}\, w(s), \qquad (4.48)$$

modulo M addition

for all $s \in \Omega$.

where

N = neighbor set appropriate to the particular model,

w_s = independent identically distributed (i.i.d) Gaussian random variable with zero mean and unit variance, characterizing noise in this model,

ρ = overall variance of the noise,

$\theta_{(i,j)}$ = real coefficients embodying the dependence of y(s) on the neighboring y values,

Weights

$\oplus$ = modulo M addition in each component

The neighbor coefficient $\theta_{(i,j)}$ can be conveniently illustrated as below.

[Ex] A neighbor set of three elements

If,

$$N = \{ s_1=(1,0),\ s_2=(0,1),\ s_3=(1,1) \}$$

Then the following tableau displays the neighbor coefficients at their proper locations.

$$\begin{array}{cccc}
0 & 0 & 0 & 0 \\
0 & \text{"1"} & -\theta_{(0,1)} & 0 \\
0 & -\theta_{(1,0)} & -\theta_{(1,1)} & 0 \\
0 & 0 & 0 & 0
\end{array}$$

Explanation

1. The θ's are entered with a minus sign to correspond to (4.48)

modified to have the θ terms on the left side.

2. The "1" is not a neighbor coefficient, but rather indicates (0,0) position.
3. All entries beyond those shown are zeros.
4. Although this example restricits the neighbor coefficients to one quadrant, this need not be the case. They may extend into a half-plane (unilateral or half-space causal model) or even into all directions (non-unilateral or non-causal model).

If a SAR model is based on this neighbor set, in order that the resulting y(s) have finite variance, the coefficients $\theta_{(k,l)}$, where $(k,l)\varepsilon N$, must obey the following condition: The eigenvalues of the transformation $B(\theta)$ from the y(s) to the w(s) must be nonzero. See for example [4] for some relevant discussion.

4.2) SYNTHETIC GENERATION OF 2-D SAR MODELS

The model as in Eq.(4.48) is perhaps the most basic one which captures stochastic spatial interactions among neighbors in a lattice. Although basic, it already looks fairly complicated if one considers using it for synthesis. Fortunately there already exist good algorithms for such procedures.

Rewriting (4.48),

$$y(s) - a = \sum_{(i,j)\varepsilon N} \theta_{(i,j)}\{y(s\oplus(i,j)) - a\} + \sqrt{\rho}\, w(s), \tag{4.49}$$

for all $s\varepsilon\Omega$.

Then we have observation set $y(s)$ obeying a SAR model.

The transformation between the observed intensities y_s and the random variable w_s can be expressed as,

$$B(\theta)\,[\,\underline{y} - a\,\underline{1}\,] = \sqrt{\rho}\ \underline{w} \tag{4.50}$$

$$(\underline{y} - a\underline{1}) = B^{-1}(\theta)\sqrt{\rho}\,\underline{w} = \Sigma(\quad)\rho\,\underline{w}$$

where $B(\theta)$ is a linear transformation matrix from the noise variates to the observations, and y, w are M^2 x 1 vectors of lexicographically ordered arrays of $\{y(.)\}$ and $\{w(.)\}$, as illustrated for y below.

$$\underline{y} = (y_{00}, y_{01}, \cdots, y_{0,M-1}, y_{10}, y_{11}, \cdots, y_{M-1,M-1})^T$$

Eq.(4.50) shows the relation between y and w. They can be considered to be random vectors related by a linear transformation matrix B. The transformation matrix B has a complicated form, namely block-circulant. Its precise structure is determined by the neighbor set N and the coefficients $\theta_{(i,j)}$.

For synthetic generation, it is necessary to assign specific values to the $\theta_{m,n}$ and ρ, and then compute the eigenvalues of matrix B, denoted by λ_{ij}. These are given in [4], for example, as

$$\lambda_{ij} = 1 - \sum_{(m,n)\varepsilon N} \theta_{m,n} \exp \left\{ \sqrt{-1} \; \frac{2\pi(im + jn)}{M} \right\} \tag{4.51}$$

Then the following formula yields the synthesis of the images obeying the SAR model as given in Eq.(4.49).

$$\underline{y} - a\underline{1} = \frac{1}{M^2} \sum_{i=0}^{M-1} \sum_{j=0}^{M-1} \underline{f}_{ij} \, \lambda_{ij}^{-1} \, (\underline{f}_{ij}^{*})^T \, \underline{w} \sqrt{\rho} \tag{4.52}$$

where

vectors are encoded in lexicographic order of the subscripts, and

f_{ij} = Fourier vectors with the (Mm + n + 1)th component given by

$$\exp \left\{ \sqrt{-1} \; 2\pi \frac{im + jn}{M} \right\} , \tag{4.53}$$

w = vector of i.i.d. Gaussian random variable distributed as N(0,1),

λ_{ij} = eigenvalues of the transformation from $\underline{y}$ to $\underline{w} \sqrt{\rho}$ as given in (4.51).

Though (4.52) looks quite simple, actual calculation can be seen to involve a large amount of computation even for fairly small images. With the use of FFT, however, calculation becomes rather fast. Detailed discussions will be given in chapter 7.

4.3) MLE AND DECISION CRITERION

1-D AR Model

For a one-dimensional autoregressive model, let N_0 be the set of relative locations which have neighbor coefficients θ_s. Then it can be written as

$$w_t = y_t - \theta_0 - \sum_{s \varepsilon N_0} y_{t-s}\theta_s \tag{4.54}$$

Thus

$$\alpha = [\phi \quad \rho]^T = [\theta_0 \; \theta_1 \quad \ldots \quad \theta_{k-1} \; \rho]^T$$

where

$$\phi = [\theta_0 \; \theta_1 \; . \; . \quad \theta_{k-1}]^T$$

So the number of parameters is $n_k = k + 1$.

Differentiating,

$$- \nabla_\phi w_t = [1 \quad y_{t-1}\ y_{t-2}\ y_{t-3} \cdots \qquad y_{t-k+1}]^T \tag{4.55}$$

Then by Eq.(3.34) with (4.55), the MLE is given as below

$$\sum_{t=1}^{m} w_t \nabla_\phi w_t = \underline{0}$$

$$\sum_{t=1}^{m} (y_t - \theta_0^* - \sum_{s\varepsilon N} y_{t-s}\, \theta_s^*)\ [\nabla_\phi w_t] = \underline{0} \tag{4.56}$$

Therefore

$$\sum_t y_t\ [\nabla_\phi w_t] = \sum_t (\theta_0^* + \sum_s \theta_s^*\, y_{t-s})\ [\nabla_\phi w_t] \tag{4.57}$$

Rewriting in vector form using Eq.(4.55)

$$- \sum_t y_t\ [\nabla_\phi w_t] = \sum_t \sum_s [\nabla_\phi w_t]\ [\nabla_\phi w_t]^T\ \theta_s^* \tag{4.58}$$

So, the MLE is given by

$$\phi^* = [\ \sum_t [\nabla_\phi w_t]\ [\nabla_\phi w_t]^T\ ]^{-1} \sum_t [\nabla_\phi w_t](-y_t) \tag{4.59}$$

And

$$\rho^* = \frac{1}{m} \sum_t w_t^2 \qquad (4.60)$$

where w_t is given by (4.54).

A decision criterion for each model hypothesis can be derived by Eq.(3.46). For actual calculation, it is more convenient to compute

$\rho^* S_m(\alpha_k^*)$ instead of $S_m(\alpha_k^*)$ itself.

Because

$$S_m(\alpha_k^*) = \frac{1}{m\rho^*} \sum_t [\nabla_\phi w_t] [\nabla_\phi w_t]^T , \qquad (4.61)$$

θ^* can be expressed as

$$\theta^* = [m \rho^* S_m(\alpha_k^*)]^{-1} \sum_t [\nabla_\phi w_t] (-y_t)$$

$$= [\rho^* S_m(\alpha_k^*)]^{-1} \frac{1}{m} \sum_t [-\nabla_\phi w_t] (y_t) \qquad (4.62)$$

Then by Eq.(3.46), the decision criterion for k-th hypothesis can be written as

$$\ln p(y_s|H_k) \simeq \frac{-m+2+(n_k-1)}{2} \ln \rho^* + \frac{-n_k}{2} \ln \frac{m}{2\pi} + \frac{\ln 2}{2}$$

$$+ \frac{-m}{2} \ln(2\pi+1) + \frac{-1}{2} \ln \det[\rho^* S_m(\alpha_k^*)] + \ln f_k(\alpha_k^*) \qquad (4.63)$$

2-D SAR Model

A two-dimensional[6] autoregressive model can be written as

$$w_{r,c} = y_{r,c} - \theta_{00} - \sum_i \sum_j y_{r-i,c-j}\, \theta_{ij} \qquad (i+j \neq 0,\ i,j \geq 0) \qquad (4.64)$$

Thus

$$\alpha = [\phi \quad \rho]^T = [\theta_{00}\ \theta_{01} \cdots \theta_{0,k-1}\ \theta_{10} \cdots \theta_{k-1,k-1} \quad \rho]^T \qquad (4.65)$$

where

$$\phi = [\theta_{00}\ \theta_{01} \ \cdots \qquad \theta_{k-1,k-1}]^T$$

So the number of parameters is $n_k = k^2 + 1$.

---

[6] Throughout this thesis, m will represent the number of samples regardless of the dimension. In other words, for a 2-D M by M image, m is the substitute for M^2.

We proceed very much as before in the one-dimensional case. Differentiating,

$$\nabla_{\phi} w_{r,c} = [-1 \quad -y_{r,c-1} \quad -y_{r,c-2} \quad \cdots \quad -y_{r-k+1,c-k+1}]^T \tag{4.66}$$

The MLE condition from Eq.(3.34) is

$$\sum_{r,c} w_{r,c} [\nabla_{\phi} w_{r,c}] = \underline{0}$$

So,

$$\sum_{r,c}^{m} (y_{r,c} - \theta^*_{00} - \sum_i \sum_j y_{r-i,c-j} \theta^*_{ij}) [\nabla_{\phi} w_{r,c}] = \underline{0} \tag{4.67}$$

Thus

$$\sum_{r,c} y_{r,c}[\nabla_{\phi} w_{r,c}] = \sum_{r,c} \{ \sum_i \sum_j \theta^*_{ij} y_{r-i,c-j} + \theta^*_{00} \} [\nabla_{\phi} w_{r,c}]$$

$$= \sum_{r,c} \{ -[\nabla_{\phi} w_{r,c}]^T \theta^* \} [\nabla_{\phi} w_{r,c}] \tag{4.68}$$

Rearranging (4.68)

$$\sum_{r,c} y_{r,c} [\nabla_\phi w_{r,c}] = \sum_{r,c} \{-[\nabla_\phi w_{r,c}][\nabla_\phi w_{r,c}]^T\} \theta^* \tag{4.69}$$

So finally

$$\theta^* = [\sum_{r,c} [\nabla_\phi w_{r,c}][\nabla_\phi w_{r,c}]^T]^{-1} \sum_{r,c} [\nabla_\phi w_{r,c}] (-y_{r,c}) \tag{4.70}$$

Also

$$S_m(\alpha_k^*) = \frac{1}{m\rho^*} \sum_{r,c} [\nabla_\phi w_{r,c}][\nabla_\phi w_{r,c}]^T \tag{4.71}$$

Combining (4.70) and (4.71) results in

$$\theta^* = [m\, \rho^*\, S_m(\alpha_k^*)]^{-1} \sum_{r,c} [\nabla_\phi w_{r,c}] (-y_{r,c})$$

And from the MLE condition

$$\rho^* = \frac{1}{m} \sum_{r,c} w_{r,c}^2 \tag{4.72}$$

The decision criterion for k-th hypothesis is

$$\ln p(y_{r,c}|H_k) = \frac{-m+2+(n_k-1)}{2} \ln \rho^* + \frac{-n_k}{2} \ln \frac{m}{2\pi} + \frac{\ln 2}{2}$$

$$+ \frac{-m}{2} \ln(2\pi+1) + \frac{-1}{2} \ln \det[\rho^* S_m(\alpha_k^*)] + \ln f_k(\alpha_k^*) \qquad (4.73)$$

where m is the number of sample points, i.e. M^2 in this M by M 2-D case.

4.4) EXAMPLES

The following examples illustrate use of the preceding theory. They are presented in order of complexity.

<u>Hypothesis:</u> 1-D H_{10}[7]

This hypothesis is a 1-D autoregressive model with neighborhood consisting of only one location, i.e. the central location. Note that this meaning of neighborhood differs from the definition of N, which excludes the central location. This model can be expressed as

$$w_t = y_t - \theta_0 \tag{4.74}$$

$\alpha_k = [\phi \quad \rho]^T = [\theta_0 \quad \rho]^T$. Thus $n_k = 2$.

$\nabla_\phi \, w_t = [\ -1\ ]$

$$S_m(\alpha_k^*) = \frac{1}{m\rho^*} \sum_{t=1}^{m} 1 = \frac{1}{\rho^*}$$

---

7 1-D autoregressive model with 1-pixel neighborhood which is central location.

Thus

$$\theta_0^* = \frac{1}{m} \sum_{t=1}^{m} y_t$$

$$\rho^* = \frac{1}{m} \sum_{t=1}^{m} w_t^2 = \frac{1}{m} \sum_{t=1}^{m} (y_t - \theta_0^*)^2$$

Therefore by (4.63), the decision criterion for this hypothesis is

$$\ln p(y_s | H_{10}) \approx \frac{-m+3}{2} \ln \rho^* - \ln \frac{m}{2\pi} + \frac{\ln 2}{2}$$

$$+ \frac{-m}{2} \ln(2\pi + 1) + \ln f_k(\alpha_k^*) \tag{4.75}$$

<u>Hypothesis:</u> 1-D H_{20}[8]

$$w_t = y_t - \theta_1 y_{t-1} - \theta_0 \tag{4.76}$$

$\alpha_k = [\ \theta_0\ \ \theta_1\ \ \rho\ ]^T$, thus $n_k = 3$

---

[8] This hypothesis is a 1-D autoregressive model with neighborhood consisting of two locations.

$$\nabla_\phi w_t = [\ -1 \quad -y_{t-1}\ ]^T$$

$$S_m(\alpha_k^*) = \frac{1}{m\rho^*} \sum_{t=1}^{m} \begin{bmatrix} 1 & y_{t-1} \\ y_{t-1} & y_{t-1}y_{t-1} \end{bmatrix}$$

Then by Eq.(4.62)

$$\theta^* = [\ \theta_0^* \quad \theta_1^*\ ]^T = [\rho^*\ S_m(\alpha_k^*)]^{-1} \frac{1}{m} \sum_{t=1}^{m} \begin{bmatrix} y_t \\ y_{t-1}y_t \end{bmatrix}$$

$$\rho^* = \frac{1}{m} \sum_{t=1}^{m} (\ y_t - \theta_0^* - \theta_1^*\ )^2$$

Finally the decision criterion is

$$\ln p(y_s|H_{20}) \approx \frac{-m+4}{2} \ln \rho^* + \frac{-3}{2} \ln \frac{m}{2\pi} + \frac{\ln 2}{2}$$

$$+ \frac{-m}{2} \ln(2\pi+1) + \frac{-1}{2} \ln (\overline{y_{t-1}^2} - \overline{y_{t-1}}^{\,2}) + \ln f_k(\alpha_k^*) \tag{4.77}$$

where
$$\overline{y_{t-1}} = \frac{1}{m} \sum_{t=1}^{m} y_{(t-1)\mathrm{Mod}\ m}$$

Hypothesis: 1-D H_{30}[9]

$$w_t = y_t - \theta_0 - \theta_1 y_{t-1} - \theta_2 y_{t-2} \tag{4.78}$$

$$\alpha_k = [\ \theta_0 \ \ \theta_1 \ \ \theta_2 \ \ \rho\ ]^T , \quad \text{thus } n_k = 4$$

$$\nabla_\phi w_t = [\ -1 \ \ -y_{t-1} \ \ -y_{t-2}\ ]^T$$

$$S_m(\alpha_k^*) = \frac{1}{m\rho^*} \sum_{t=1}^{m} [\nabla_\phi w_t][\nabla_\phi w_t]^T$$

Therefore MLE can be written as

$$\theta^* = [\rho^* \ S_m(\alpha_k^*)]^{-1} \frac{1}{m} \sum_{t=1}^{m} \begin{bmatrix} y_t \\ y_{t-1} \\ y_{t-2} \end{bmatrix}$$

$$\rho^* = \frac{1}{m} \sum_{t=1}^{m} (\ y_t - \theta_0^* - \theta_1^*\ y_{t-1} - \theta_2^*\ y_{t-2}\ )^2$$

9 This hypothesis is a 1-D autoregressive model with neighborhood consisting of two locations.

Finally the decision criterion is

$$\ln p(y_s|H_{30}) \simeq \frac{-m+5}{2} \ln \rho^* - 2 \ln \frac{m}{2\pi} + \frac{\ln 2}{2} + \frac{-m}{2} \ln(2\pi+1)$$

$$+ \frac{-1}{2} \ln \det[\rho^* S_m(\alpha_k^*)] + \ln f_k(\alpha_k^*) \tag{4.79}$$

<u>Hypothesis:</u> 2-D H_{00}[10]

This is similar to 1-D H_{00} except the number of samples m is now the substitute for M^2, i.e. the number of samples of a M by M image. See Eq.(3.47).

So the decision criterion is

$$\ln p(y_{r,c}|H_{00}) \simeq \frac{-m+2}{2} \ln \rho^* - 2 \ln \frac{m}{2\pi} + \frac{\ln 2}{2}$$

$$+ \frac{-m}{2} \ln(2\pi+1) + \ln f_k(\alpha_k^*) \tag{4.80}$$

---

[10] This hypothesis is a trivial autoregressive model with no neighborhood.

Hypothesis: 2-D H_{10}[11]

THis is similar to 1-D H_{10} except m is the substitute for M^2, i.e. the number of samples of a M by M image. See Eq.(4.75).

The decision criterion is

$$\ln p(y_{r,c}|H_{10}) \simeq \frac{-m+3}{2} \ln \rho^* - \ln \frac{m}{2\pi} + \frac{\ln 2}{2}$$

$$+ \frac{-m}{2} \ln(2\pi + 1) + \ln f_k(\alpha_k^*) \tag{4.81}$$

Hypothesis: 2-D H_{20}[12]

$$w_{r,c} = y_{r,c} - \theta_{00} - \theta_{01} y_{r,c-1} - \theta_{10} y_{r-1,c} - \theta_{11} y_{r-1,c-1} \tag{4.82}$$

$\alpha_k = [\ \theta_{00}\ \theta_{01}\ \theta_{10}\ \theta_{11}\ \ \rho\ ]^T$, thus $n_k = 5$

[11] This hypothesis is a 2-D simultaneous autoregressive model with neighborhood consisting of one location.

[12] This hypothesis is a 2-D simultaneous autoregressive model with 2 by 2 neighborhood.

$$\nabla_\phi w_{r,c} = [\ -1 \quad -y_{r,c-1} \quad -y_{r-1,c} \quad -y_{r-1,c-1}\ ]^T$$

$$S_m(\alpha_k^*) = \frac{1}{m\rho^*} \sum_r \sum_c [\nabla_\phi w_{r,c}]\ [\nabla_\phi w_{r,c}]^T$$

So the MLE is given by

$$\theta^* = [\ \rho^*\ S_m(\alpha_k^*)\ ]^{-1} \frac{1}{m} \sum_r \sum_c \begin{bmatrix} y_{r,c} \\ y_{r,c}y_{r,c-1} \\ y_{r,c}y_{r-1,c} \\ y_{r,c}y_{r-1,c-1} \end{bmatrix}$$

$$\rho^* = \frac{1}{m} \sum_r \sum_c (y_{r,c} - \theta_{00} - \theta_{01}y_{r,c-1} - \theta_{10}y_{r-1,c} - \theta_{11}y_{r-1,c-1})^2$$

Finally, the decision criterion is

$$\ln p(y_{r,c}|H_{20}) = \frac{-m+6}{2} \ln \rho^* + \frac{-5}{2} \ln \frac{m}{2\pi} + \frac{\ln 2}{2} + \ln f(\alpha_k^*)$$

$$+ \frac{-m}{2} (\ln 2\pi + 1) + \frac{-1}{2} \ln \det[\rho^*\ S_m(\alpha_k^*)] \qquad (4.83)$$

CHAPTER 5. POLYNOMIAL REGRESSIVE MODEL HYPOTHESIS

5.1) DEFINITION AND SYNTHESIS

Definition: Polynomial regressive model[13] can be defined as below.

For 1-D model,

$$y_t = \sum_{j=0}^{k} a_j t^j + w_t , \quad n_k = k + 2 \tag{5.84}$$

For 2-D model, Coordinates

$$y_{r,c} = \sum_{i=0}^{k-1} \sum_{j=0}^{k-1} a_{ij} r^i c^j + w_{r,c} , \quad n_k = k^2 + 1 \tag{5.85}$$

where

w_t or $w_{r,c}$ is an i.i.d. noise term with variance ρ and mean 0.

Synthesis: Each $y_{r,c}$ value is just a simple function of coordinates, r and c. So the synthesis of this model is rather straightforward compared to the synthesis of autoregressive model.

[13] When the model is local, i.e. it applies to an area representing a facet of a 3-D object, some authors call it simply facet model.

5.2) MLE AND DECISION CRITERION

1-D model

The polynomial regression models have coefficients a_0, a_1, ... associated with the respective terms. The hypothesis H_{01}, having only a_0 as coefficient, is identical to the hypothesis H_{10}, the random field model with only θ_0 as coefficient. The next hypotheses have increasing numbers of a's.

The general form is given by

$$w_t = y_t - \sum_j a_j t^j \tag{5.86}$$

By Eq.(3.34), the MLE is given by

$$\sum_t (y_t - \sum_j a_j^* t^j) [\nabla_\phi w_t] = \underline{0} \tag{5.87}$$

$$\sum_t y_t [\nabla_\phi w_t] = \sum_t \sum_j a_j^* t^j [\nabla_\phi w_t] . \tag{5.88}$$

Because

$$\phi = [a_0 \; a_1 \; \ldots \quad a_k]^T ,$$

$$\nabla_{\phi} w_t = [\ -1 \quad -t \quad -t^2 \ . \ . \ . \quad -t^k\ ]^T = -\underline{t}^T$$

Then, Eq.(5.88) can be expressed in vector form

$$-\sum_t \underline{t}\, y_t = \sum_t [\nabla_{\phi} w_t]\ \underline{t}^T\ \underline{a}^* \tag{5.89}$$

$$\sum_t \underline{t}\, y_t = \sum_t \underline{t}\ \underline{t}^T\ \underline{a}^* \tag{5.90}$$

$$\underline{a}^* = [\ \sum_t \underline{t}\ \underline{t}^T\ ]^{-1} \sum_t \underline{t}\ y_t \tag{5.91}$$

By the MLE condition,

$$\rho^* = \frac{1}{m} \sum_t {w_t}^2 \tag{5.92}$$

Then by Eq.(3.46), the decision criterion for k^{th} hypothesis is given as

$$\ln p(y_s|H_k) = \frac{-m + 2 + (n_k - 1)}{2} \ln \rho^* + \frac{-n_k}{2} \ln \frac{m}{2\pi} + \frac{\ln 2}{2}$$

$$+ \frac{-m}{2} \ln\ (2\pi+1) + \frac{-1}{2} \ln \det[\rho^*\ S_m(\alpha_k)] + \ln f_k(\alpha_k^*) \tag{5.93}$$

where n_k is the number of parameters, and

$$S_m(\alpha_k^*) = \frac{1}{m\rho^*} \sum_t [\nabla_\phi w_t] [\nabla_\phi w_t]^T$$

2-D Model

2-D polynomial regression model can be written as

$$w_{r,c} = y_{r,c} - \sum_{i=0}^{k-1} \sum_{j=0}^{k-1} a_{ij} r^i c^j \tag{5.94}$$

Therefore

$$\alpha = [\phi \quad \rho]^T = [a_{00} \; a_{01} \quad \ldots \quad a_{k-1,k-1} \quad \rho \;]^T$$

So, $n_k = k^2 + 1$

$$\nabla_\phi w_{r,c} = [\; -1 \quad -c \quad -c^2 \; \ldots \; -c^{k-1} \quad -r \quad -rc \; \ldots \; -r^{k-1} c^{k-1} \;]^T$$

By Eq.(3.34), the MLE is given by

$$\sum_{r,c} (\; y_{r,c} - \sum_i \sum_j a_{ij} r^i c^j \;) \; [\nabla_\phi w_{r,c}] = \underline{0}$$

Rewriting in vector form,

$$\sum_{r,c} y_{r,c}[\nabla_\phi w_{r,c}] = \sum_{r,c} [\nabla_\phi w_{r,c}][\nabla_\phi w_{r,c}]^T (-\underline{a}^*)$$

where

$$\underline{a}^* = [\ a^*_{00}\ a^*_{01}\ a^*_{02}\ \ldots\ a^*_{k-1,k-1}\ ]^T = \phi^*$$

So

$$\underline{a}^* = [\ \sum_{r,c} [\nabla_\phi w_{r,c}][\nabla_\phi w_{r,c}]^T\ ]^{-1} \sum_{r,c} (-y_{r,c})[\nabla_\phi w_{r,c}] \tag{5.95}$$

$$\rho^* = \frac{1}{m} \sum_r \sum_c w^2_{r,c} \tag{5.96}$$

Then by Eq.(3.46), decision criterion for k^{th} hypothesis is

$$\ln p(y_{r,c}|H_k) = \frac{-m + 2 + (n_k - 1)}{2} \ln \rho^* + \frac{-n_k}{2} \ln \frac{m}{2\pi} + \frac{\ln 2}{2}$$

$$+ \frac{-m}{2} \ln (2\pi+1) + \frac{-1}{2} \ln \det[\rho^* S_m(\alpha_k)] + \ln f_k(\alpha^*_k) \tag{5.97}$$

where n_k is the number of parameters, and

$$S_m(\alpha_k^*) = \frac{1}{m\rho^*} \sum_{r,c} [\nabla_\phi w_{r,c}] [\nabla_\phi w_{r,c}]^T$$

Detailed examples are given in next section.

5.3) EXAMPLES

The following examples illustrate use of the preceding theory. They are presented in order of complexity.

Hypothesis: 1-D H_{01}[14]

$$w_t = y_t - a_0 \tag{5.98}$$

This is the same hypothesis as 1-D H_{10}. See Eq.(4.75) for decision criterion of this hypothesis.

Hypothesis: 1-D H_{02}[15]

$$w_t = y_t - a_0 - a_1 t \tag{5.99}$$

$$\alpha = [\ a_0 \quad a_1 \quad \rho\ ]^T \text{ , so } n_k = 3$$

---

[14] 1-D 1-coefficient polynomial model

[15] 1-D 2-coefficient polynomial model

$$\nabla_{\phi} w_t = [\ -1 \quad -t\ ]^T = -\underline{t}$$

$$S_m(\alpha_k^*) = \frac{1}{m\rho^*} \sum_t [\nabla_{\phi} w_t]\ [\nabla_{\phi} w_t]^T$$

$$= \frac{1}{m\rho^*} \sum_t \begin{bmatrix} 1 & t \\ t & t^2 \end{bmatrix}$$

But for m odd,

$$\sum_t t = 0 \qquad , \text{ for } \quad t \le \left| \frac{m-1}{2} \right| \tag{5.100}$$

$$\sum_t t^2 = \frac{m(m-1)(m+1)}{12} \qquad , \text{ for } \quad t \le \left| \frac{m-1}{2} \right|$$

Then with (5.100),

$$S_m(\alpha_k^*) = \frac{1}{\rho^*} \begin{bmatrix} 1 & 0 \\ 0 & \frac{(m-1)(m+1)}{12} \end{bmatrix}$$

So,

$$\det [\ \rho^* \ S_m(\alpha_k^*)\ ] = \frac{(m-1)(m+1)}{12} \simeq \frac{m^2}{12}$$

By Eq.(5.91) and Eq.(5.92)

$$\underline{a}^* = [\sum_t \underline{t}\ \underline{t}^T]^{-1} \sum_t y_t\ [1\quad t]^T = [a_0^*\quad a_1^*]^T$$

$$\rho^* = \frac{1}{m} \sum_t w_t^2$$

Finally the decision criterion for this hypothesis is

$$\ln p(y_s|H_{02}) = \frac{-m+4}{2} \ln \rho^* + \frac{-3}{2} \ln \frac{m}{2\pi} + \frac{\ln 2}{2}$$

$$+ \frac{-m}{2} (\ln 2\pi+1) + \frac{-1}{2} \ln \frac{m^2-1}{12} + \ln f_k(\alpha_k^*) \qquad (5.101)$$

<u>Hypothesis:</u> 1-D H_{03}[16]

$$w_t = y_t - a_0 - a_1 t - a_2 t^2 \qquad (5.102)$$

$$\alpha_k = [\ a_0\quad a_1\quad a_2\quad \rho\ ]^T \text{, so } n_k = 4$$

---

[16] 1-D 3 coefficient polynomial model

$$\nabla_{\phi} w_t = [\ -1 \quad -t \quad -t^2\ ]^T = -\underline{t}$$

$$S_m(\alpha_k^*) = \frac{1}{m\rho^*} \sum_t \begin{bmatrix} 1 & t & t^2 \\ t & t^2 & t^3 \\ t^2 & t^3 & t^4 \end{bmatrix}$$

As before,

$$\sum_t t = 0 \qquad \text{and} \qquad \sum_t t^3 = 0$$

$$\sum_t t^2 = \frac{m(m-1)(m+1)}{12} \qquad , \text{ for } \quad t \le \left| \frac{m-1}{2} \right|$$

$$\sum_t t^4 = \frac{(m^2 - 1)\, m\, (3m^2 - 7)}{240} \simeq \frac{m^5}{80}$$

With the above information,

$$\det [\ \rho^* S_m(\alpha_k^*)\ ] \simeq \frac{m^6}{2160}$$

By Eq.(5.91) and Eq.(5.92)

$$\underline{a}^* = [\ \rho^* S_m(\alpha_k^*)\ ]^{-1} \frac{1}{m} \sum_t y_t \begin{bmatrix} 1 \\ t_2 \\ t^2 \end{bmatrix}$$

$$\rho^* = \frac{1}{m} \sum_t w_t^2$$

The decision criterion is

$$\ln p(y_s|H_{03}) = \frac{-m+5}{2} \ln \rho^* - 2 \ln \frac{m}{2\pi} + \frac{\ln 2}{2}$$

$$+ \frac{-m}{2} \ln (2\pi+1) + \frac{-1}{2} \ln \det[\rho^* S_m(\alpha_k)] + \ln f_k(\alpha_k^*) \qquad (5.103)$$

<u>Hypothesis:</u> 2-D H_{02}[17]

$$w_{r,c} = y_{r,c} - a_{00} - a_{01}c - a_{10}r - a_{11}rc \qquad (5.104)$$

$$\alpha_k = [\ a_{00}\ a_{01}\ a_{10}\ a_{11}\ \ \rho\ ]^T\ ,\ \text{so } n_k = 5$$

$$\nabla_\phi\, w_{r,c} = [\ -1\ \ -c\ \ -r\ \ -rc\ \ ]^T$$

By definition,

---

[17] 2-D 2nd order polynomial model

$$\rho^* S_m(\alpha_k^*) = \frac{1}{m} \sum_r \sum_c [\nabla_\phi w_{r,c}] [\nabla_\phi w_{r,c}]^T$$

As derived before,

$$\sum_r \sum_c r\, c = 0 \,, \qquad \frac{1}{M^2} \sum_c \sum_r r^2 = \frac{1}{M^2} \sum_r \sum_c c^2 \approx \frac{M^2}{12} = \frac{m}{12}$$

where m is the substitute for M^2, the number of samples of a M by M sized image.

So, the MLE of coefficients and variance are by Eq.(5.91) and Eq.(5.92)

$$\underline{a}^* = [\ \rho^* S_m(\alpha_k^*)\ ]^{-1} \frac{1}{m} \sum_{r,c} y_{r,c} [\ 1 \quad c \quad r \quad rc\ ]^T$$

$$\rho^* = \frac{1}{m} \sum_{r,c} w_{r,c}^{\,2}$$

The decision criterion is,

$$\ln p(y_{rc}|H_{02}) = \frac{-m+6}{2} \ln \rho^* + \frac{-5}{2} \ln \frac{m}{2\pi} + \frac{\ln 2}{2}$$

$$+ \frac{-m}{2} \ln (2\pi+1) + \frac{-1}{2} \ln \det[\rho^* S_m(\alpha_k)] + \ln f_k(\alpha_k^*) \qquad (5.105)$$

5.4) DISCUSSION

In general, for a polynomial model with n_k parameters, we have $(n_k - 1)$ coefficients, since variance is one of the parameters. Then the degree of polynomial is $(n_k - 2)$ for the 1-D model. Assuming it to be even, we can evaluate det[$S_m(\alpha_k^*)$] to be of order

$$\prod_{j=0}^{n_k-2} (m^2)^j \, (\rho^*)^{-1} = (\rho^*)^{-(n_k-1)} \prod_{j=0}^{n_k-2} m^{2j} \tag{5.106}$$

Then - (1/2) ln det[$S_m(\alpha_k^*)$] is approximately of order

$$\frac{n_k-1}{2} \ln \rho^* + \frac{-1}{2} (n_k-1)(n_k-2) \ln m$$

We can see that for m large, Eq.(3.46) becomes

$$\ln p(y_s | H_k)$$

$$\simeq \frac{-m+2}{2} \ln \rho^* + \frac{-m}{2} (\ln 2\pi + 1) + \frac{-n_k}{2} \ln \frac{m}{2\pi} + \frac{\ln 2}{2}$$

$$+ \frac{-1}{2} \ln \det[S_m(\alpha_k^*)] + \ln f_k(\alpha_k^*)$$

$$\simeq \frac{-m+n_k+1}{2} \ln \rho^* + \frac{-1}{2} (n_k^2 - 2n_k + 2) \ln m + \frac{-m}{2}$$

$$- \left(\frac{m - n_k}{2}\right) \ln 2\pi + \frac{\ln 2}{2} + \ln f_k(\alpha_k^*) \qquad (5.107)$$

So, we conclude that the major penalty for an overparameterized polynomial model is a punishing $(-(1/2)\, n_k^2 \ln m)$ term.

CHAPTER 6. COMPOSITE MODEL HYPOTHESIS

6.1) MLE AND DECISION CRITERION

1-D Model

Two possible versions of a combined model are as below. They differ in that the first has polynomial terms within the autoregressive part, and the second does not.

$$y_t - \sum_j a_j t^j = \sum_{s\varepsilon N} \theta_s \{ y_{t-s} - \sum_l a_l (t-s)^l \} + w_t \tag{6.108}$$

$$y_t = \sum_{s\varepsilon N} \theta_s y_{t-s} + \sum_l a_l t^l + \theta_0 + w_t \quad , (l,s \neq 0) \tag{6.109}$$

AR poly

Though (6.108) and (6.109) are actually equivalent, the second form is more convenient for development of estimation.

Rewriting (6.109),

$$w_t = y_t - \theta_0 - \sum_{s\varepsilon N} \theta_s y_{t-s} - \sum_l a_l t^l \quad , (l,s \neq 0) \tag{6.110}$$

Then by Eq.(3.34), the MLE is given by

$$\sum_{t} (y_t - \sum_{s=1}^{k_1-1} \theta_s^* y_{t-s} - \sum_{l=1}^{k_2-1} a_l^* t^l - \theta_0^*) [\nabla_\phi w_t] = 0$$

$$\alpha = \begin{bmatrix} \phi \\ - \\ \rho \end{bmatrix} = [\theta_0 \ \theta_1 \cdots \theta_{k_1-1} \ a_1 \ a_2 \ \cdots \ a_{k_2-1} \ \ \rho]^T$$

So, $n_k = k_1 + k_2$, and

$$\nabla_\phi w_t = [\ -1 \ -y_{t-1} \ \cdots \ -y_{t-k_1+1} \ \ -t \ -t^2 \ \ldots \ -t^{k_2-1} \ ]^T$$

In vector form,

$$\sum_{t} y_t [\nabla_\phi w_t] = \sum_{t} [\nabla_\phi w_t] [\nabla_\phi w_t]^T (-\phi^*)$$

Thus,

$$\phi^* = [\sum_{t} [\nabla_\phi w_t][\nabla_\phi w_t]^T]^{-1} \sum_{t} [\nabla_\phi w_t] (-y_t) \tag{6.111}$$

With those estimates, w_t is determined. Also by the MLE condition,

$$\rho^* = \frac{1}{m} \sum_{t} w_t^2 \tag{6.112}$$

Because

$$S_m(\alpha_k^*) = \frac{1}{m\rho^*} \sum_t [\nabla_\phi w_t] [\nabla_\phi w_t]^T$$

$$\phi^* = [\rho^* S_m(\alpha_k^*)]^{-1} \frac{1}{m} \sum_t [-\nabla_\phi w_t] y_t \tag{6.113}$$

Eq.(6.113) is more convenient than Eq.(6.111) for actual calculation.

Finally the decision criterion is

$$\ln p(y_s|H_{k_1k_2}) \approx \frac{-m+2+(k_1+k_2-1)}{2} \ln \rho^* + \frac{-(k_1+k_2)}{2} \ln \frac{m}{2\pi}$$

$$+ \frac{-m}{2} \ln (2\pi+1) + \frac{\ln 2}{2} + \ln f(\alpha_k^*) + \frac{-1}{2} \ln \det[\rho^* S_m(\alpha_k^*)] \tag{6.114}$$

2-D Model

Let us continue on to the 2-D model. This is straightforward generalization of the 1-D model.

$$w_{r,c} = y_{r,c} - \theta_{00} - \sum_i \sum_j \theta_{ij} y_{r-i,c-j} - \sum_l \sum_m a_{lm} r^l c^m \tag{6.115}$$

where $l,m \neq 0$ and $i,j \neq 0$.

$$\alpha = [\ \theta_{00}\ \theta_{01}\ \cdots\ \theta_{k_1-1,k_1-1}\quad a_{01}\ a_{02}\ \cdots\ a_{k_2-1,k_2-1}\quad \rho\ ]^T$$

So, $n_k = k_1^{\ 2} + k_2^{\ 2}$

$$\nabla_\phi\, w_{r,c} = [\ -1\ -y_{r,c-1}\ \cdots\ -y_{r-k_1+1,c-k_1+1}\quad -c\ -c^2\ \ldots\ -r^{k_2-1} c^{k_2-1}\ ]^T$$

Then, by Eq.(3.34), the MLE is expessed in vector form as

$$\sum_{r,c} y_{r,c}\, [\nabla_\phi\, w_{r,c}] = \sum_{r,c} [\nabla_\phi\, w_{r,c}]\ [\nabla_\phi\, w_{r,c}]^T\ (-\phi^*)$$

Therefore,

$$\phi^* = [\theta^*_{00}\ \theta^*_{01}\ \cdots\ \theta^*_{k_1-1,k_1-1}\ \cdots\ a^*_{01}\ a^*_{02}\ \cdots\ a^*_{k_2-1,k_2-1}]^T$$

$$= [\ \sum_{r,c} [\nabla_\phi\, w_{r,c}]\ [\nabla_\phi\, w_{r,c}]^T\ ]^{-1} \sum_{r,c} [-\nabla_\phi\, w_{r,c}]\ y_{r,c} \qquad (6.116)$$

Then MLE for variance is given as below using parameters derived in (6.116).

$$\rho^* = \frac{1}{m} \sum_{r,c} w_{r,c}^2 \qquad , m = \text{number of samples} \tag{6.117}$$

Recalling

$$S_m(\alpha_k^*) = \frac{1}{m\rho^*} \sum_{r,c} [\nabla_\phi w_{r,c}][\nabla_\phi w_{r,c}]^T$$

Using above expressions, MLE can be written as

$$\phi^* = [\rho^* S_m(\alpha_k^*)]^{-1} \frac{1}{m} \sum_{r,c} [-\nabla_\phi w_{r,c}] y_{r,c} \tag{6.118}$$

Eq.(6.118) is more convenient for actual computation. Then the decision criterion is,

$$\ln p(y_{r,c}|H_{k_1,k_2})$$

$$\simeq \frac{-1}{2} \{m-2-(k_1^2+k_2^2-1)\} \ln \rho^* + \frac{-(k_1^2+k_2^2)}{2} \ln \frac{m}{2\pi} + \frac{-m}{2} (\ln 2\pi+1)$$

$$+ \frac{\ln 2}{2} + \frac{-1}{2} \ln \det[\rho^* S_m(\alpha_k^*)] + \ln f(\alpha_k^*) \tag{6.119}$$

6.2) EXAMPLES

The following examples illustrate use of the preceding theory. They are presented in order of complexity.

Hypothesis: 1-D H_{22}

$$w_t = y_t - \theta_0 - \theta_1 y_{t-1} - a_1 t \tag{6.120}$$

$$\alpha = [\ \phi \quad \rho\ ]^T = [\ \theta_0\ \theta_1\ a_1\ \rho\ ]^T, \qquad n_k = 4$$

$$\nabla_\phi w_t = [\ -1 \quad -y_{t-1} \quad -t\ ]^T$$

By Eq.(6.111) and (6.113),

$$\phi^* = [\ \sum_t [\nabla_\phi w_t][\nabla_\phi w_t]^T\ ]^{-1} \sum_t [\nabla_\phi w_t]\ (-y_t)$$

$$= [\ \rho^* S_m(\alpha_k^*)\ ]^{-1} \frac{1}{m} \sum_t \begin{bmatrix} y_t \\ y_{t-1} y_t \\ t\ y_t \end{bmatrix}$$

$$\rho^* = \sum_t (y_t - \theta_0^* - \theta_1^* y_{t-1} - a_1^* t)^2$$

where

$$S_m(\alpha_k^*) = \frac{1}{m\rho^*} \sum_t \begin{bmatrix} 1 & y_{t-1} & t \\ y_{t-1} & y_{t-1}y_{t-1} & t\, y_{t-1} \\ t & t\, y_{t-1} & t^2 \end{bmatrix}$$

With this information, the decision criterion is

$$\ln p(y_s|H_{22}) \simeq \frac{-m+7}{2} \ln \rho^* - 2 \ln \frac{m}{2\pi} + \frac{-m}{2} \ln (2\pi + 1)$$

$$+ \frac{\ln 2}{2} + \ln f(\alpha_k^*) + \frac{-1}{2} \ln \det[\rho^* S_m(\alpha_k^*)] \tag{6.121}$$

<u>Hypothesis:</u> 2-D H_{00}

$$w_{r,c} = y_{r,c} \tag{6.122}$$

See example in chapter 5.

<u>Hypothesis:</u> 2-D H_{11} ($= H_{10} = H_{01}$)

$$w_{r,c} = y_{r,c} - \theta_{00} \tag{6.123}$$

$$\alpha = [\ \theta_{00}\ \ \rho\ ]^T, \qquad \text{thus } n_k = 2$$

$$\nabla_\phi w_{r,c} = -1$$

$$S_m(\alpha_k^*) = \frac{1}{m\rho^*} \sum_{r,c} 1 = \frac{1}{\rho^*}$$

$$\phi^* = \theta_{00}^* = \frac{1}{m} \sum_{r,c} y_{r,c}$$

$$\rho^* = \frac{1}{m} \sum_{r,c} (y_{r,c} - \theta_{00}^*)^2$$

Then by Eq.(6.119), the decision criterion is

$$\ln p(y_{r,c}|H_{11}) \simeq \frac{-m+3}{2} \ln \rho^* - \ln \frac{m}{2\pi} + \frac{\ln 2}{2}$$

$$+ \frac{-m}{2} (\ln 2\pi + 1) + \ln f(\alpha_k^*) \tag{6.124}$$

Hypothesis: 2-D H_{21} (= H_{20})

Because we combined constant terms of SAR model and polynomial model into one, there is no meaning for $k_2 = 1$. So all the procedures are same as 2-D H_{20}. See example in chapter 4.

Hypothesis: 2-D H_{12} (= 2-D H_{02})

By definition, the model for H_{12} is

$$w_{r,c} = y_{r,c} - \theta_{00} - a_{01}c - a_{10}r - a_{11}rc \tag{6.125}$$

And for H_{02} is

$$w_{r,c} = y_{r,c} - a_{00} - a_{01}c - a_{10}r - a_{11}rc \tag{6.126}$$

The only difference is the notation of the constant term. So they can be treated as equivalent. For details refer to example in Chapter 5.

Hypothesis: 2-D H_{22}

$$\begin{aligned} w_{r,c} = y_{r,c} - \theta_{00} - \theta_{01}y_{r,c-1} - \theta_{10}y_{r-1,c} - \theta_{11}y_{r-1,c-1} \\ - a_{01}c - a_{10}r - a_{11}\,rc \end{aligned} \tag{6.127}$$

$$\alpha = [\ \theta_{00}\ \theta_{01}\ \theta_{10}\ \theta_{11}\ a_{01}\ a_{10}\ a_{11}\ \rho\ ]^T \quad , n_k = 8$$

$$\nabla_\phi w_{r,c} = [\ -1 \quad -y_{r,c-1} \quad -y_{r-1,c} \quad -y_{r-1,c-1} \quad -c \quad -r \quad -rc\ ]^T$$

$$S_m(\alpha_k^*) = \frac{1}{m\rho^*} \sum_{r,c} [\nabla_\phi w_{r,c}][\nabla_\phi w_{r,c}]^T$$

$$\phi^* = [\rho^* S_m(\alpha_k^*)]^{-1} \frac{1}{m} \sum_{r,c} [-\nabla_\phi w_{r,c}]\ y_{r,c}$$

$$= [\ \rho^* S_m(\alpha_k^*)\ ]^{-1} \frac{1}{m} \sum_{r,c} \begin{bmatrix} y_{r,c} \\ y_{r,c}y_{r,c-1} \\ y_{r,c}y_{r-1,c} \\ y_{r,c}y_{r-1,c-1} \\ c\ y_{r,c} \\ r\ y_{r,c} \\ r\ c\ y_{r,c} \end{bmatrix}$$

$$\rho^* = \frac{1}{m} \sum_{r,c} [\ w_{r,c}(\phi^*)\ ]^2 \qquad , m = \text{number of samples}$$

Then the decision criterion is

$$\ln p(y_{r,c}|H_{22}) \ = \ \frac{-m+9}{2} \ln \rho^* - 4 \ln \frac{m}{2\pi} + \frac{-m}{2} (\ln 2\pi + 1)$$

$$+ \frac{\ln 2}{2} + \frac{-1}{2} \ln \det[\rho^{*} S_m(\alpha_k^{*})] + \ln f(\alpha_k^{*}) \qquad (6.128)$$

CHAPTER 7. APPLICATIONS AND RESULTS OF EXPERIMENTS

7.1) SYNTHESIS AND ESTIMATION

Polynomial Model

Synthesis

We used an existing GIPSY[18] command, called SURFAC, to generate polynomial images. Using SURFAC, we can adjust size, order, and parameters of an image. The synthesized image has integer-valued pixels.

To add noise to the generated image, we used the GIPSY command NOISE. With NOISE, we can control the mean and variance of added noise.

Estimation

To estimate the parameters of the given image with the knowledge of model hypothesis, all we have to do is just the implementation of Eq.(5.95).

Because we tried only square images, programming was rather straightforward except for a few steps such as dealing with even sized images. But

---

[18] General Image Processing SYstem --- the special system developed and used by the Spatial Data Analysis Laboratory of Virginia Tech for handling the multi-dimensional data [23].

theoretically speaking, estimation of non-square images is also possible. More details will be mentioned in section 3, where merging is discussed.

Experimental Results

Figure 1 shows some typical polynomial images:

(a) 1st order with $y(r,c) = 15 + 2r + c$.

(b) With noise $N(0,4)$ added to (a).

(c) 2nd order with $y(r,c) = .2r + .5c + .1rc$.

(d) With noise $N(0,8)$ added to (c).

Table 1 shows estimated parameters of the 4 images given in Figure 1.

Figure 2 shows images generated with estimated parameters:

(a) is for Figure 1 (a).

(b) is for Figure 1 (b).

(c) is for Figure 1 (c).

(d) is for Figure 1 (d).

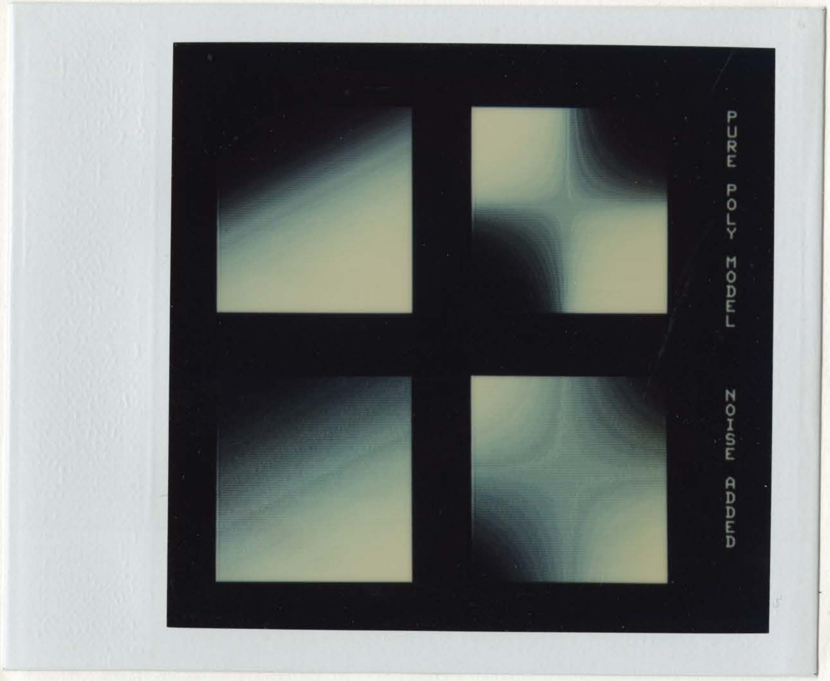

a c
b d

Figure 1. Some synthesized polynomial images: a)upper left - 1st order pure polynomial b) lower left - same plus noise c)upper right - 2nd order pure polynomial d)lower right - same plus noise

Table 1. Estimated parameters of 4 images shown in Fig. 1.

Figure	rho		A00		A01		A10		A11	
	true	est'ed	true	est'ed	true	est'ed	true	est'ed	true	est'ed
a	0.0	0.01	15.0	15.0	1.0	1.0018	2.0	2.0015	0.0	-0.000
b	16.0	16.036	15.0	15.017	1.0	0.9996	2.0	2.0001	0.0	-0.000
c	0.0	0.0789	0.0	0.0015	0.5	0.4997	0.2	0.1999	0.1	0.0999
d	64.0	64.045	0.0	0.0335	0.5	0.4987	0.2	0.1997	0.1	0.0999

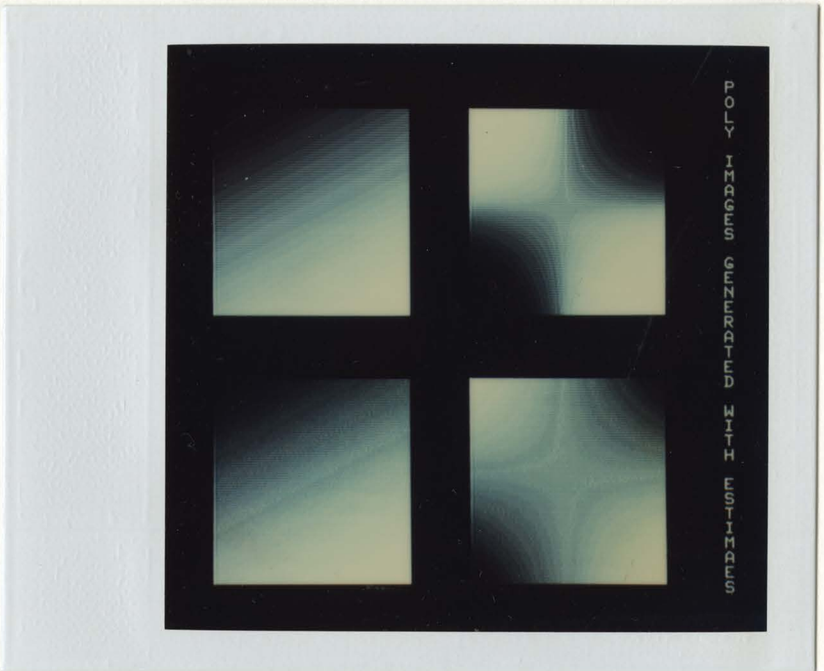

a | c
b | d

Figure 2. Polynomial images generated with estimated parameters of Figure 1: Each of a) b) c) d) is for a) b) c) d) of Figure 1.

AR Model

Synthesis

To implement the Eq.(4.52), the formula for generating SAR images, we made several GIPSY commands. The sequence of commands to generate one such image is given in Figure 3.

Each command name and its function is described below.

FFTNO

input --- pure noise image (in our experiment)

output --- 2-D FFT version of noise image

function --- performs 2-D FFT with variety of input images

FFTNEB

input --- no image, just parameters

output --- 2-D FFT version of pure SAR images without noise

function --- generates variety of pure SAR images

MULT

input --- output of FFTNO and FFTNEB

ouput --- multiplied image of two inputs

function --- performs pixel by pixel multiplication

INVFFT

input --- output of MULT

output --- SAR image with noise added

function --- performs inverse FFT to make
a desired image

Estimation

In this thesis, we estimate the parameters of 2 x 2 neighborhood or 3 x 3 neighborhood images. Because we assume toroidal lattice for the coordinate grid, the input image to be estimated has no boundary conditions. Also, if we have enough samples, we can determine both parameter values and the neighbor scheme without any prior information. That is, we can not only estimate the parameter values but also can find, with asymptotic consistency, the model hypothesis. More details on identification will be discussed in section 2 of this chapter.

```
 ------------------
| image of constant |
|    pixel value    |
 ------------------                     desired parameter values
        |                                ----------------------
        | NOISE                                    |
        |  (variance                               | FFTNEB
        |   specified)                             |
        |                                 ----------------------
 -----------------                       |  Fourier transformed  |
| pure noise image |                     |     neighborhood      |
 -----------------                        ----------------------
        |                                          |
        | FFTNO                                    |
        |                                          |
 ---------------------                             |
| Fourier transformed |                            |
|    noise image      |                            |
 ---------------------                             |
         |                                         |
            ----------------------------------------
                      |
                      | MIXER
                      |
            ----------------------------------
           |  Fourier transformed SAR image   |
           |       with noise added           |
            ----------------------------------
                      |
                      | INVFFT
                      |  (add mean value)
                      |
             ----------------
            |  desired image |
             ----------------
```

Figure 3. Sequence of GIPSY commands to generate SAR image

Experimental Results

Figure 4 shows some SAR images with a variety of parameter values:

(a) 2 x 2 neighborhood with s(1,0)=.9, s(0,1)=.9, and w = N(0,4).

(b) 2 x 2 neighborhood with s(1,0)=-.5, s(0,1)=.6, s(1,1)=.3, and w = N(0,4).

(c) 3 x 3 neighborhood with s(1,0)=-.7, s(2,0)=-.3, s(0,1)=.73, s(0,2)=-.1, s(1,1)=.25, s(1,2)=-.1, and w = N(0,3.8).

(d) 3 x 3 neighborhood with s(0,1)=.34, s(1,0)=.1, s(1,1)=.21, s(2,2)=.3, and w = N(0,3.255).

Table 2 shows the estimated parameter values of images given in Figure 4 as well as true values. Note that case (a) can not be estimated well by our approximate MLE formulas, because the determinant term in the likelihood is not negligible. In fact, the transfer function

$$(1 - .9z_1^{-1} - .9z_2^{-1})^{-1}$$

is actually unstable on an infinite lattice. It has pole at $z_1 = 1.8$, $z_2 = 1.8$, for example. This differs from

$$[(1 - .9z_1^{-1}) (1 - .9z_2^{-1})]^{-1},$$

which is stable with poles close to the unit circle.

Figure 5 shows images generated with estimated parameter values:

(a) is for Figure 4 (a)

(b) is for Figure 4 (b)

(c) is for Figure 4 (c)

(d) is for Figure 4 (d)

To the eye, cases (b), (c), (d) appear to be successfully estimated and resynthesized. For case (a), in spite of the totally different estimates, the resynthesized image has almost the same pattern as the original one except for the slightly higher frequency.

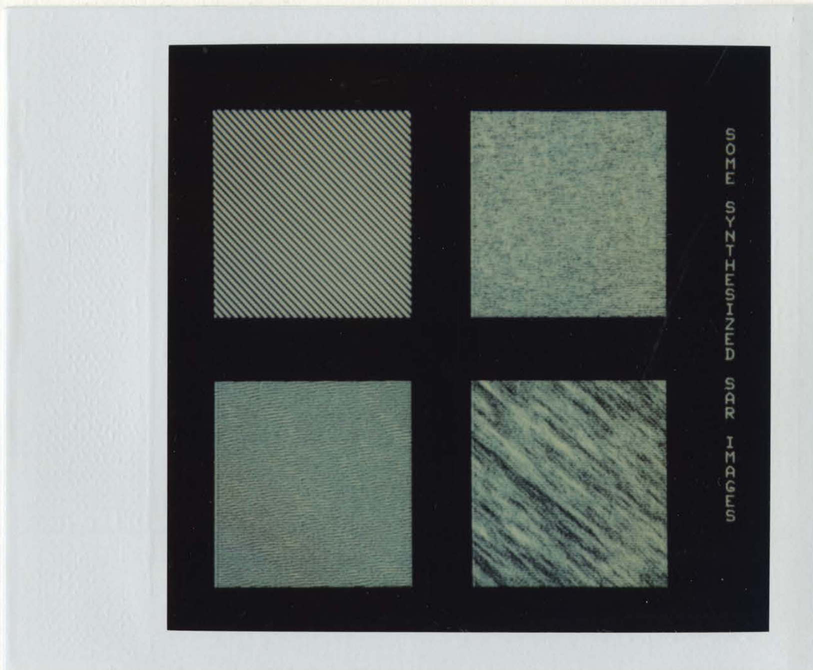

2x2 a | c 3x3

2x2 b | d 3x3

Figure 4. Some synthesized SAR images: a) is a typical example whose determinant term is not negligible. b) c) d) are images to which our algorithm is readily applicable.

Table 2. Estimated parameter of images given in Figure 4.

Figure	rho = Var		a(0,0)		a(0,1)		a(1,0)		a(1,1)	
	true	est'ed	true	est'ed	true	est'ed	true	est'ed	true	est'ed
a	16.0	1998.3	10.0	9.953	0.9	1.0993	0.9	1.0996	0.0	-1.207
b	16.0	16.047	10.0	10.047	0.6	0.5911	-.5	-.4991	0.3	0.2979
c	14.5	15.385	10.0	10.045	0.73	0.7103	-.7	-.7026	0.25	0.2686
d	10.6	11.254	9.97	10.427	0.34	0.3402	0.1	0.1068	0.21	0.2175

Figure	a(0,2)		a(1,2)		a(2,0)		a(2,1)		a(2,2)	
	true	est'ed	true	est'ed	true	est'ed	true	est'ed	true	est'ed
a	0.0	-.972	0.0	1.099	0.0	-.9724	0.0	1.071	0.0	-.9498
b	0.0	0.0	0.0	0.0	0.0	0.0	0.0	0.0	0.0	0.0
c	-.1	-.093	-.1	-.089	-.3	-.3125	0.0	0.0	0.0	0.0
d	0.0	0.0	0.0	0.0	0.0	0.0	0.0	0.0	0.3	0.2845

00 01 02
10 11 12
20 21 22

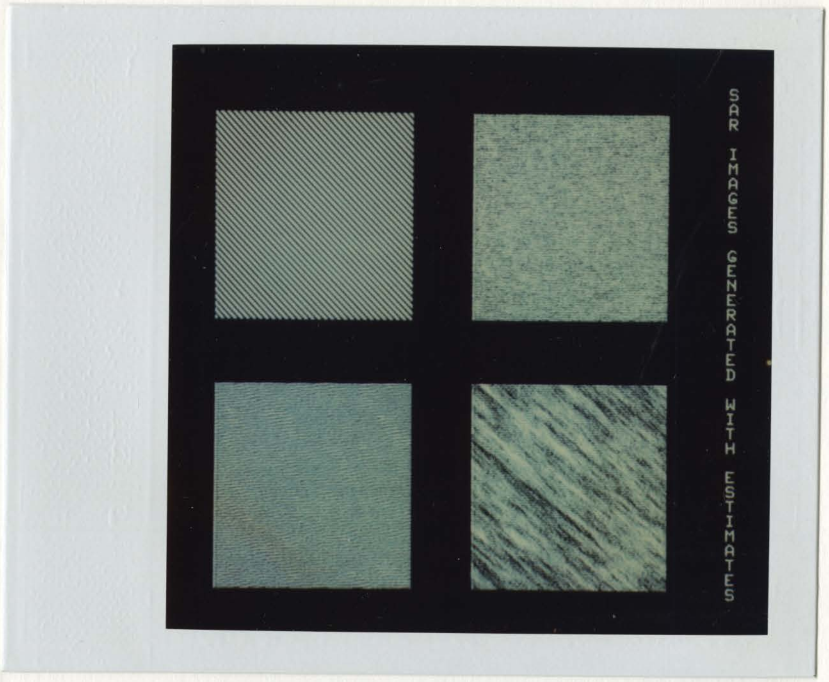

Figure 5. SAR images generated with estimated parameters of Figure 4: Each of a) b) c) d) is for a) b) c) d) of Figure 4.

7.2) MODEL IDENTIFICATION

Algorithm

Model identification can be treated as the extension of estimation problem. In other words, model identification is done by general decision criterion which exploits the estimated parameter values.

Given a test image, it is hypothesized to be one of several classes of images such as 1st order polynomial or 2nd order polynomial or 2 x 2 neighborhood SAR or 3 x 3 neighborhood SAR image. Each hypothesis has its own decision criterion calculated from the given test image. Then we decide that the given image belongs to a certain class which gives the maximum value of decision criterion.

During the calculation of the decision criterion for each hypothesis, we already computed the estimated parameters of the test image assuming that this image belongs to this specific model class. So as mentioned in Section 7.1), we can also give MLE parameter values of the test image as a byproduct of this process.

This algorithm is briefly illustrated by block diagram in Figure 6.

```
                 ---------------
                | subject image |
                 ---------------
                        |
                 -----------------
                | hypothesized as |
                 -----------------
                        |
  -----     -----     -----     -----     -----     ------
 | Hoo |   | Ho1 |   | Ho2 |   | H2o |   | H3o |   | H22  |
 |     |   | H11 |   | H12 |   | H21 |   | H31 |   |  (not
 |     |   | H1o |   |     |   |     |   |     |   |   implemented)
  -----     -----     -----     -----     -----     ------
    |         |         |         |         |
   ----------------------------------------
  |      estimate  parameters  for         |
  |          each hypothesis               |
   ----------------------------------------
                      |
                      |
   -----------------------------------------
  | calculate decision criterion for        |
  |          each hypothesis                |
  |       |       |       |         |       |
  | D     | D     | D     | D       | D     |
  |  i1   |  i2   |  i3   |  i4     |  i5   |
   -----------------------------------------
                      |
                      |
         --------------------
        |   find Max. D_i    |
         --------------------
                      |
                      |
     -------------------------------
    |    image is identified as     |
    |   belong to the model which   |
    | gives Max. decision criterion |
     -------------------------------
```

Figure 6. Block diagram of model identification algorithm

Experimental Results

Table 3. shows the decision criterion value of several hypotheses for given test images. The model hypotheses with detailed parameters are as follows.

1) H_{00}: image of pure noise distributed as N(0,1).
2) H_{01}: image of constant pixel gray-level value 9.
3) H_{02}: 1.0+1.0c+1.0r+3.0rc + N(0,9)
4) H_{02}: 0.5+0.8c+0.2r+0.1rc
5) H_{20}: 10.+0.5y(r-1,c)+0.8y(r,c-1)+0.4y(r-1,c-1) + N(0,4)
6) H_{30}: 10.+0.5y(r-1,c)+0.6y(r,c-1)+0.3y(r-1,c-1)
   +0.2y(r-2,c-1) + N(0,4)

According to our experiments, the decision criterion almost always selects the correct model. This is expected from the procedure's theoretical consistency. Table 4 summarizes the results of repeated experiments.

Table 3. Decision criterion of each hypothesis for given test images

true model	decision criterion for each hypothesis: H00	H01	H02	H20	H30	selected model
H00	-5922.	-5925.	-5945.	-5933.	-6105.	H00
H01	-14810.	23163.	23121.	13034.	12555.	H01
H02	-34200.	-34196.	-15246.	-17481.	-22319.	H02
H02	-20693.	-20691.	-658.	-3465.	-9055.	H02
H20	-68282.	-51980.	-52020.	-43678.	-44150.	H20
H30	-68502.	-53436.	-53473.	-45104.	-43826.	H30

Table 4. Comparison of true vs. identified model

true model	identified model H00	H01	H02	H20	H30	total test images	percent of accuracy *
H00	5					5	100 %
H01		5				5	100 %
H02			10			10	100 %
H00				8		8	100 %
H30				1	4	5	80 %
							96.7 %

* Note : Tests have been done only a small number of times. So the derived percent of accuracy does not imply the overall perfomance.

Discussion

Image identification is the extension of estimation, but it is also a special case of image segmentation procedure which is the topic of the next section. In other words, image identification can be treated as a special case of segmentation such that the whole image is segmented as one uniform region.

So, in the computer implementation, we did not generate a specific GIPSY command for image identification alone. Instead, we can use the command which is for segmentation for this purpose with specific user-specified inputs. More details will be discussed in section 7.3).

7.3) SEGMENTATION

There are two ways of segmenting an image: by delineating the boundaries surrounding its region, or by defining its homogeneous regions directly. Obviously if we can do one perfectly then we also do the other perfectly. But the processing methods of the two procedures are quite different. We will only be concerned with those techniques that define regions directly. We followed a strategy which falls within the so-called split-and-merging approaches for extracting and defining the regions. The test image is initially split into pieces and later merged into several big regions by a kind of homogeneity test. More details are given below.

Description of Procedures

As mentioned before, segmentation is the extension of image identification and estimation. In other words, segmentation algorithm can use ML estimates and general decision criterion as its powerful tools. The following is a brief description of our segmentation algorithm.

a) First, we split the test image into several blocks of reasonable size. We can vary this initial splitting size easily as an user input. Unless the size of test image, say M by M, is quite small, the desirable initial block size is somewhere around square root of M.

b) For those initially split blocks, we calculate their decision criteria, identify models, and estimate parameter values.

c) The first candidates of blocks to be merged are those which have small rho (=variance) values, among the blocks not yet merged.

d) We attempt to merge neighboring blocks according to a comparison of decision criterion values for a merged hypothesis vs. an unmerged hypothesis.

e) Finally, the mergeable blocks have been combined into larger regions, and the unmergeable blocks are left by themselves.

The procedure was applied to the following kinds of test images:

First, ideal test images synthesized by us.

Second, ideal image as an object
natural image[19] as background.

Third, natural image as an object
ideal image as background.

Table 5 summarizes the composition and shape of our test images. The real and arbitrary shaped objects should be the next target of our experiments.

---

19 Images from Brodatz textures [19] have been used in our experiments.

Table 5. Composition and shape of our test images

	Object Shape	Object Model	Background Model	Refer to Figure.
1.	square	synth poly	synth AR	
2.	"	synth AR	synth poly	
3.	"	synth AR	synth AR	
4.	"	synth poly	synth poly	8.(b)
5.	circle	synth poly	synth AR	9.(b)
6.	"	synth AR	synth poly	
7.	"	synth AR	synth AR	8.(a)
8.	"	synth poly	synth poly	9.(a)
9.	square	synth poly	real texture	10.(a)
10.	"	real texture	synth poly	11.(b)
11.	circle	synth poly	real texture	10.(b)
12.	"	real texture	synth poly	11.(a)

Merging

At the beginning of merging, test image is divided into several square blocks by specified block size. We call this step as initial splitting. For each of these blocks, we identify its model, estimate the parameters of identified model, and compute the decision criterion. Initially we assign region number 0 to all these blocks. A sample of this initial calculation is provided in Appendix A. According to our experiments, as we can verify at Appendix A, the result of initial calculation is likely to be good enough, i.e. the calculation selects the right model and estimates accurately, unless the block size is too small. Those blocks which have border lines in them usually have high rho (=variance) values.

Then we proceed to try to merge each block with one of the neighboring blocks. The first candidate to be merged is the block whose variance is the lowest. In other words, those blocks with lower variance are more likely to be homogeneous and are more likely to be merged with surrounding blocks.

Once the candidate block is chosen, it is temporarily combined with one of the four neighboring blocks. Then we calculate the decision criterion of this combined block. If this combined decision criterion is larger than the sum of two small blocks, we merge these two blocks into one region and assign an initial region number. Otherwise they are separated again. This process continues until all four surrounding blocks have been tested.

This pairwise calculation of decision criterion keeps going until all of the blocks are tested.

During this process, we assign new region numbers to the merged blocks, and as program proceeds we may combine one big region into another region by making their region number the same. So at the end of the merging procedure, we have not only a pixel-labeled image but also a tentative list of regions. The region number of unmerged blocks remains 0, and, unlike the other region numbers, does not indicate block membership in the same region.

The algorithm so far described is compactly illustrated in Figure 7.

Experiments

We experimented with variety of compositions of models and object shapes. Here we present only some of them, as summarized in Table 5. In Figure 8 through 11, upper row shows test images and lower row shows the result of merging. As we can see, the region of polynomial model is always merged well. The region of autoregressive model is not always merged perfectly. But at least, the autoregressive model region and polynomial model region are always separated.

An interesting thing is the performance with real images, which are digitized from Brodatz texture [19]. In these examples, the accuracy of merging of real images is actually better than that of ideal synthesized images. This can be verified by referring to Figures 10 and 11.

To deal with test images with different geometries such as different object size or shape, it is possible to adjust the decision criterion according to the prior probabilities of combined blocks. If the object size is adequate and the number of boundary pixels large, then the probability of merging, P(m), will be almost same with the probability of separating, P(s). But if the object is small compared to background, then P(m) may be much higher than P(s). In this case, we should add $\ln P(m)/P(s)$ to the decision criterion for combined vs. uncombined blocks, thereby giving some weight in favor of merging. Figure 12 illustrates the effect of such an additive threshold on merging performance. Figure 13 illustrates the effect of initial splitting size. Image d) indicates that a multi-resolution approach could be beneficial.

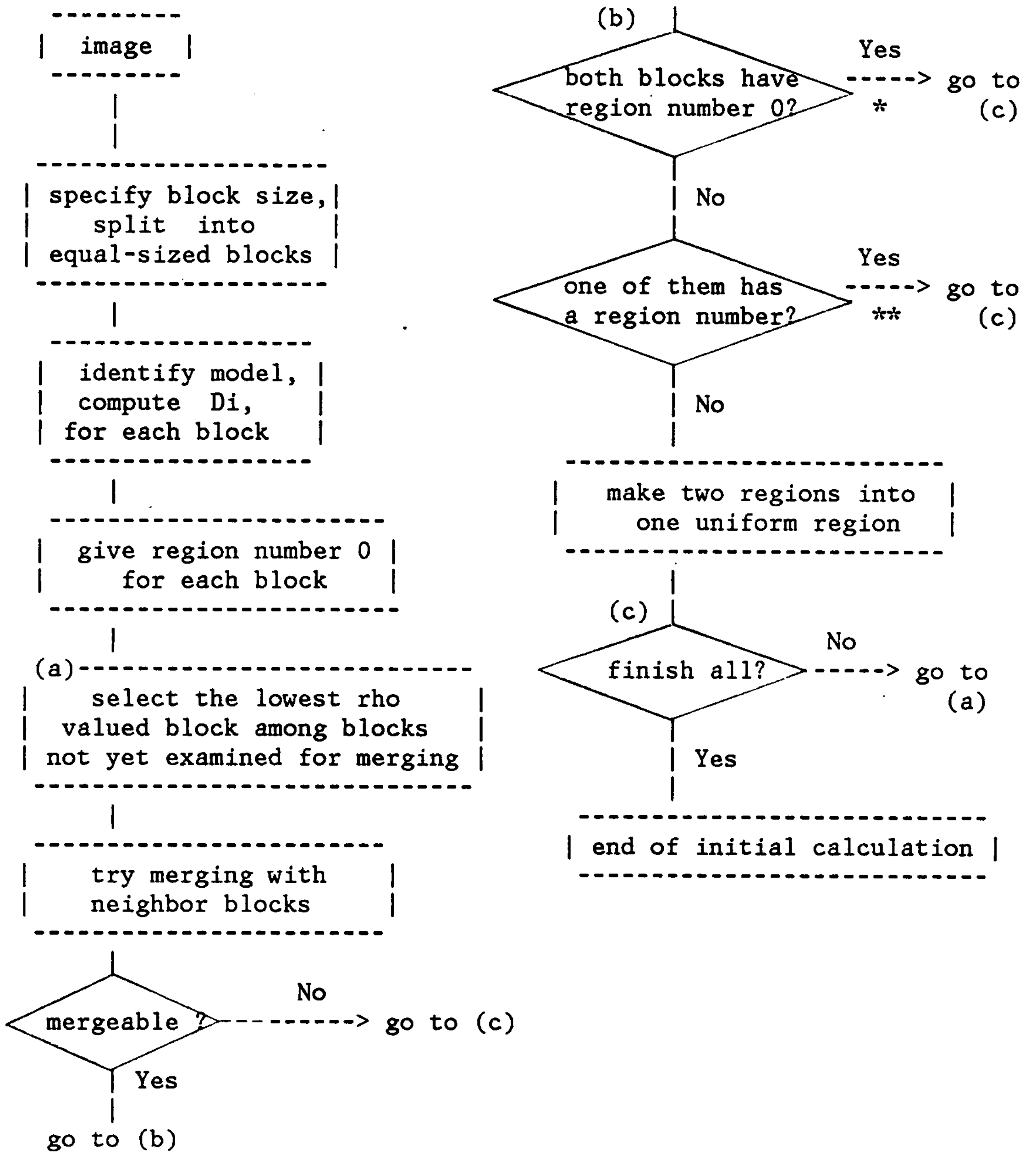

Figure 7. Block diagram of merging algorithm: * - assign a new region number to both blocks, ** - assign the region number of one to another

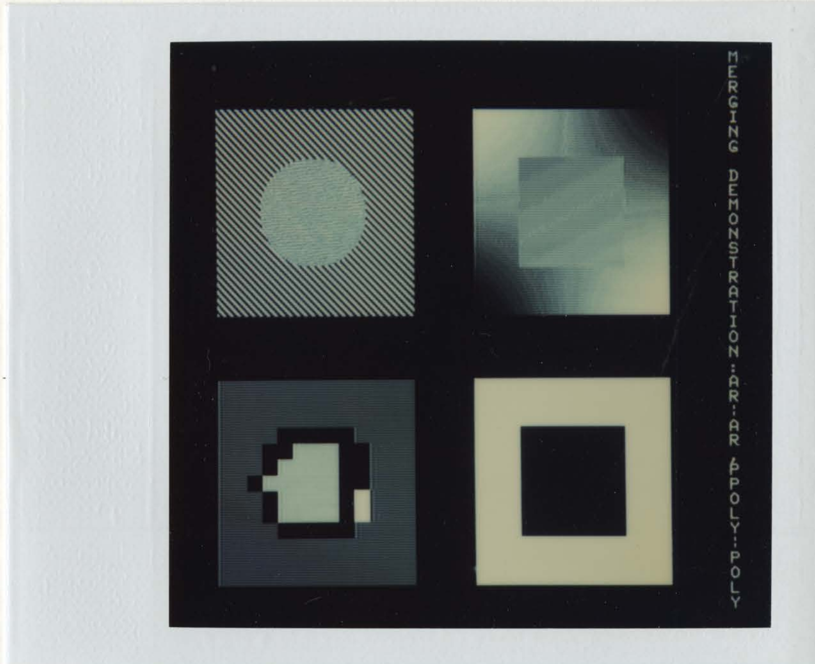

Original

merged

Figure 8. Results of merging(1): Upper row has original images, bottom row has the results of merging. Refer to Table 5 for details.

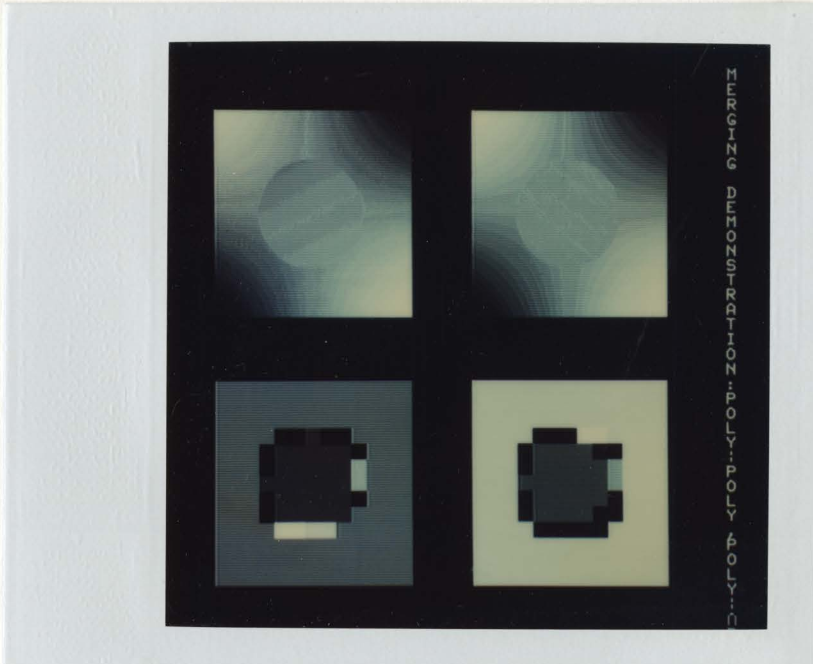

original

merged

Figure 9. Results of merging(2): Upper row has original images, bottom row has the results of merging. Refer to Table 5 for details.

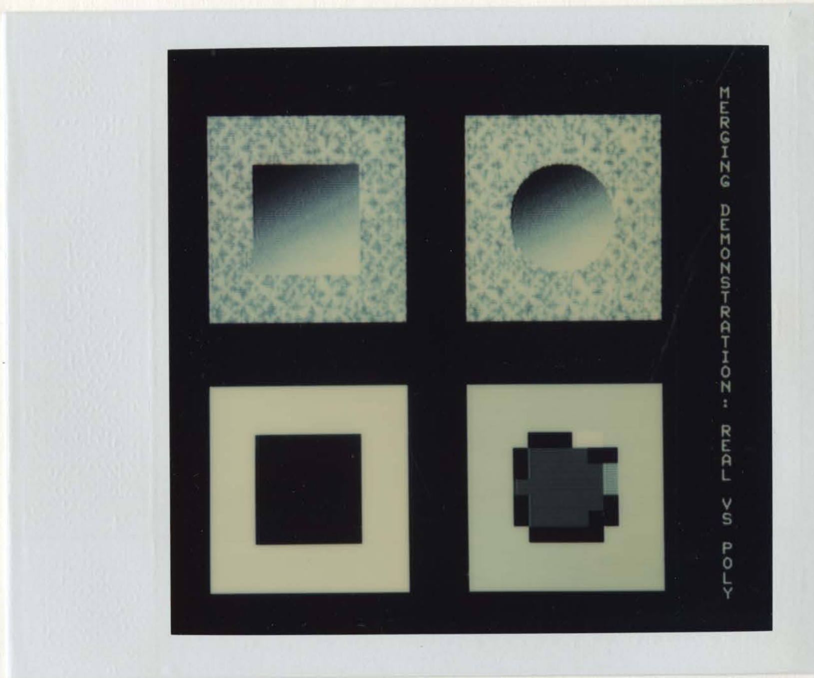

Figure 10. Results of merging(3): Upper row has original images, bottom row has the results of merging. Refer to Table 5 for details.

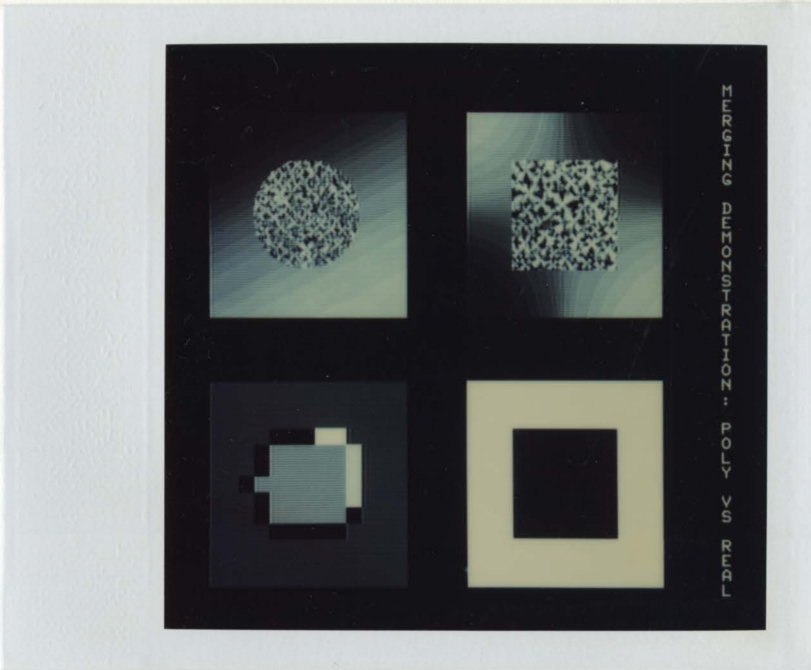

Figure 11. Results of merging(4): Upper row has original images, bottom row has the results of merging. Refer to Table 5 for details.

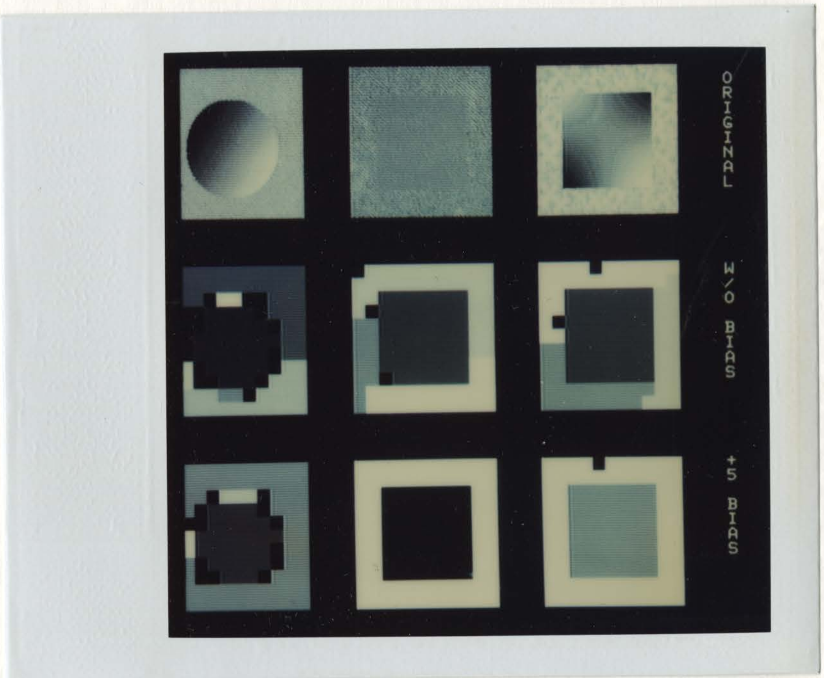

Figure 12. Effects of threshold on merging performance.: Original images are on the 1st row. The 2nd row has the results of merging without a priori weighting. Images on the 3rd row are the results of merging with weighted decision criterion.

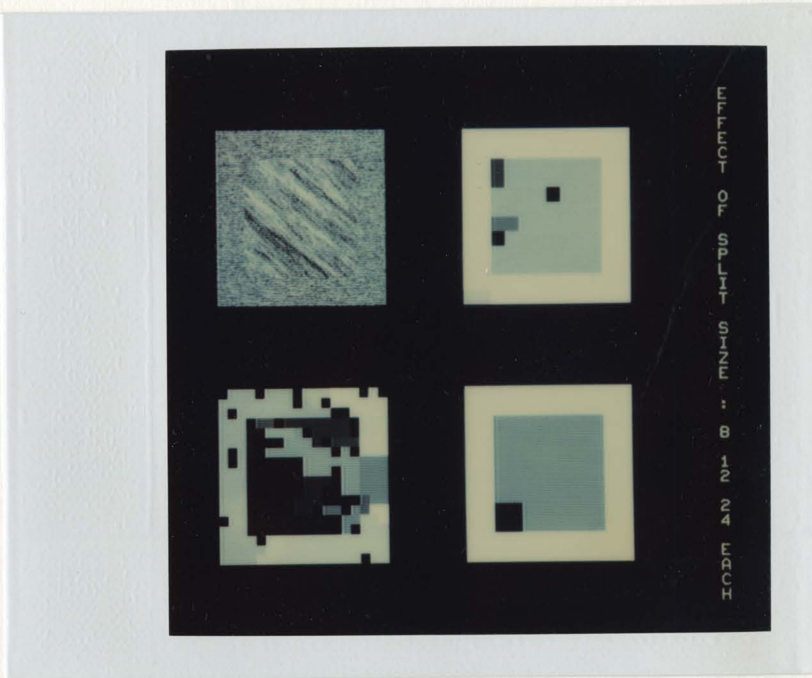

a | b 12x12

d | c 24x24

8x8

Figure 13. Effects of initial block size: From left-upper corner clockwise (a) original, (b) block size 12 x 12, (c) block size 24 x 24, (d) block size 8 x 8.

Discussion

Our segmentation scheme may be classified as a kind of split-and-merge approach. But so far most of people using this kind of approach have been dealt with the simplest images such as white object on a dark background, e.g. Milgram [20]. Others, such as Chen and Pavlidis [~~18~~16], use as their statistical tool for homogeneity testing a difference in a simple greytone property such as mean or variance. These approaches cannot accomodate the more sophisticated hypotheses explored here.

We want to mention a few strong points of our approach to segmentation.

practicability Performance with real image texture was very good.

versatility We can work with images of a variety of model hypotheses, including polynomial models, SAR random fields, and others as well.

efficiency Iteration is not much involved in the process.

CONCLUSION

We have described our unified approach to early image understanding and shown that this approach has versatility to deal with a variety of model hypotheses. It is applicable to statistical models such as polynomial or random-field ones, and others as well.

Other attractive features of our approach worth mentioning are the efficiency and practicability. Segmentation can be done with less computation and the performance with real image was quite satisfactory. One drawback may be the border line between regions that may may be less smooth than for other techniques such as pixel-labeling approaches. But that drawback may be tolerable because we can accomodate more general visual textures and model hypotheses.

A major problem of our approach during implementation was the assumption of equal prior probabilities and uniform prior distribution. Future research should be aimed at these aspects, perhaps by estimating these priors from extensive data bases of pictures. Also real images with arbitrary shaped objects in them should be the next target of our experiments.

The result of our segmentation can be a basis for the higher-level image understanding, such as by means of artificial intelligence approaches to computer vision.

We conclude that, with more research, this new approach should prove to be a comprehensive and powerful tool for early image analysis.

APPENDIX A. SAMPLE OUTPUT OF INITIAL CALCULATION.

```
Image : object - square, synthesized SAR model with AR(22)
                 y(r,c)=.6y(r,c-1)+.5y(r-1,c)+.3y(r-1,c-1) + N(0,4)
        background - synthesized polynomial model with
                 y(r,c)=2.+r+.5c+.5rc + N(0,1) Poly(2)
        size - 121 x 121 (block size - 11 x 11, 121 blocks)
(type number 2 stands for 2nd order polynomial model and type number 3
stands for 2 by 2 neighborhood SAR model)
```

ROW	COL	TYPE#	RHO	DI	A00	A01	A10	A11
1	1	3	12.0782	-327.2795	16.0875	0.4437	0.4119	0.2481
1	2	3	11.1524	-322.3105	14.8028	0.3713	0.3484	0.4240
1	3	3	14.8634	-339.4430	13.9737	0.3793	0.3130	0.4768
1	4	3	13.9811	-335.9991	14.2553	0.4572	0.2714	0.4336
1	5	3	11.1123	-322.2440	14.4722	0.4498	0.3625	0.2605
1	6	3	17.4727	-349.1556	13.5924	0.4473	0.3163	0.3825
1	7	3	14.2973	-336.6266	15.1603	0.3318	0.2715	0.3922
1	8	3	10.6073	-320.4420	14.3060	0.4627	0.3639	0.4550
1	9	3	13.1821	-332.5175	15.8264	0.4167	0.2573	0.4327
1	10	3	14.1255	-336.9022	14.7093	0.5112	0.3277	0.3477
1	11	3	13.7995	-343.1233	14.1139	0.5655	0.2956	0.3401
2	1	3	14.4283	-337.1395	14.6752	0.4250	0.2585	0.4113
2	2	3	14.1203	-336.1615	14.6873	0.3984	0.3577	0.4038
2	3	3	10.7840	-320.8941	14.9357	0.4483	0.2484	0.5180
2	4	3	14.1032	-336.7561	16.4848	0.5071	0.3188	0.3931
2	5	3	11.8317	-326.2784	14.6001	0.4691	0.4757	0.2448
2	6	3	13.7017	-333.9052	15.7506	0.3464	0.2844	0.3684
2	7	3	13.3567	-332.4402	14.8239	0.4200	0.2965	0.4264
2	8	3	14.2244	-337.1881	14.6277	0.5004	0.4002	0.3283
2	9	3	15.8267	-342.1546	14.8684	0.3533	0.2986	0.1501
2	10	3	14.6553	-337.9311	15.2474	0.4207	0.3291	0.2712
2	11	3	11.8337	-325.5924	14.7530	0.2937	0.3371	0.4559
3	1	3	15.0307	-339.3484	14.8302	0.3777	0.4391	0.1455
3	2	3	15.4312	-341.5426	15.8304	0.4632	0.2498	0.3879
3	3	2	1.2126	-194.4434	496.9752	0.9383	0.5099	0.5128
3	4	2	0.9344	-179.4608	326.3471	1.0445	0.5041	0.4909
3	5	2	1.1004	-188.8627	156.0992	1.0364	0.5256	0.4848
3	6	2	1.3146	-199.0885	-14.5124	0.9760	0.5041	0.4939
3	7	2	0.7814	-182.2832	-184.9587	1.0132	0.5107	0.5039
3	8	2	1.2419	-195.8200	-355.4463	1.0264	0.4826	0.5057
3	9	2	1.1042	-189.0626	-525.8182	0.9868	0.4818	0.5135
3	10	3	14.3384	-337.1052	12.7673	0.3267	0.2772	0.5136
3	11	3	11.1566	-322.1099	15.1980	0.3168	0.0930	0.4811
4	1	3	14.7624	-338.3120	15.2049	0.4951	0.3838	0.2900
4	2	3	12.4164	-328.4645	13.3812	0.3549	0.2529	0.4426

APPEN.LOG;1 20-MAY-1985 23:33 Page 3

4	3	2	1.2340	-195.4520	320.9091	0.9529	0.5347	0.4931
4	4	2	1.2091	-194.2802	210.8264	0.9802	0.5174	0.4918
4	5	2	1.1300	-190.3875	100.8182	1.0570	0.5421	0.5037
4	6	2	1.0377	-185.4916	-9.0744	1.0331	0.4446	0.5044
4	7	2	1.1082	-189.2692	-118.9669	0.9967	0.4992	0.4918
4	8	2	1.1252	-190.1455	-228.8347	0.9967	0.4603	0.4965
4	9	2	0.9757	-181.9496	-338.8264	0.9545	0.4471	0.5166
4	10	3	16.0581	-343.5837	13.1034	0.3596	0.1720	0.5334
4	11	3	17.7748	-349.2064	15.7378	0.4569	0.2989	0.2588
5	1	3	11.1604	-322.6567	14.1830	0.6284	0.3937	0.3378
5	2	3	16.0680	-344.1827	14.4091	0.3996	0.3274	0.4677
5	3	2	0.9692	-181.5600	144.9587	1.0421	0.5083	0.5081
5	4	2	1.0240	-184.7273	95.4132	0.9934	0.5091	0.4950
5	5	2	1.3777	-201.7858	45.9091	1.0193	0.5372	0.4919
5	6	2	1.1463	-191.2360	-3.3802	1.0198	0.5149	0.5008
5	7	2	1.3167	-199.1802	-52.7686	0.9992	0.5190	0.5042
5	8	2	1.1011	-188.8976	-102.2645	1.0065	0.5124	0.5023
5	9	2	1.1420	-190.9948	-152.0083	0.9643	0.4992	0.5157
5	10	3	18.9274	-353.7733	15.2721	0.4577	0.4633	0.3021
5	11	3	20.1413	-356.8735	15.5989	0.2737	0.3191	0.4355

(Appendix A continues)

6	1	3	16.8355	-347.1646	15.1843	0.4805	0.4216	0.4167
6	2	3	14.1153	-336.6778	14.1894	0.3580	0.3477	0.3759
6	3	2	1.0595	-188.8223	-31.0000	1.0017	0.5612	0.4859
6	4	2	0.9793	-182.1609	-20.0909	0.9583	0.5727	0.5070
6	5	2	1.0204	-186.1893	-9.1901	0.9592	0.5537	0.5127
6	6	2	1.1293	-190.3779	1.8843	1.0065	0.5083	0.4843
6	7	2	1.2155	-194.5863	13.3719	0.9863	0.4719	0.5009
6	8	2	1.2013	-193.9318	24.1488	0.9793	0.5149	0.4766
6	9	2	1.0157	-184.2565	35.1157	1.0372	0.4380	0.5036
6	10	3	13.3197	-333.0862	15.8206	0.4883	0.3011	0.3315
6	11	3	14.8784	-338.8005	13.1549	0.3921	0.2686	0.3565
7	1	3	14.2733	-337.5931	14.9259	0.3545	0.3071	0.5039
7	2	3	11.6194	-324.6587	15.4631	0.3577	0.3176	0.3748
7	3	2	1.1510	-191.4494	-207.0826	0.9534	0.5331	0.4985
7	4	2	1.1271	-190.2413	-135.4959	0.9525	0.4744	0.4987
7	5	2	1.3452	-200.4134	-63.8843	1.0438	0.4711	0.5076
7	6	2	1.2280	-195.1733	7.4380	0.9893	0.4992	0.4979
7	7	2	0.9881	-182.6736	79.0579	0.9645	0.4975	0.4999
7	8	2	0.9812	-182.2720	150.4876	0.9727	0.4901	0.5109
7	9	2	1.1462	-191.2059	222.0165	1.0000	0.5248	0.5129
7	10	3	16.9187	-346.4044	12.6511	0.3836	0.3679	0.3808
7	11	3	10.0118	-316.1502	15.8102	0.4783	0.5242	0.2667
8	1	3	14.3871	-337.6595	15.9193	0.5505	0.4006	0.2486
8	2	3	17.4197	-348.6216	14.2639	0.3713	0.2212	0.5125
8	3	2	1.0055	-183.6760	-382.8017	0.9298	0.5223	0.5003
8	4	2	0.9946	-183.0501	-250.8347	0.9719	0.5314	0.4922
8	5	2	1.1910	-193.4138	-118.8182	1.0116	0.5207	0.4958
8	6	2	1.1799	-192.8750	12.9256	1.0008	0.5306	0.5180
8	7	2	1.1218	-189.9717	144.9587	1.0339	0.5124	0.5062
8	8	2	0.9422	-179.9383	276.8843	0.9983	0.5033	0.4842
8	9	2	1.0491	-186.1155	409.0083	1.0438	0.4810	0.4948
8	10	3	13.0047	-332.2070	14.5437	0.4165	0.3006	0.5167
8	11	3	16.5595	-346.2808	14.9939	0.3814	0.2026	0.5766
9	1	3	13.6953	-333.8871	14.5234	0.4763	0.5231	0.2341
9	2	3	14.9173	-339.6299	14.5175	0.4591	0.3976	0.3499
9	3	2	1.3850	-199.5422	-558.8099	0.9711	0.4777	0.5038

9	4	2	1.0933	-188.4902	-366.3306	1.0108	0.4835	0.5011
9	5	2	1.0566	-186.5247	-173.7521	0.9686	0.5041	0.5007
9	6	2	0.9500	-182.7822	18.5702	0.9752	0.4744	0.4948
9	7	2	0.9324	-179.3382	210.7107	0.9760	0.4802	0.4944
9	8	2	1.0101	-183.9411	403.4628	1.0107	0.5843	0.4967
9	9	2	1.0791	-187.7375	595.9504	1.01[illegible]1	0.5099	0.4949
9	10	3	14.7264	-338.4131	14.6439	0.4610	0.3148	0.3475
9	11	3	10.9048	-321.1631	15.3971	0.3898	0.2340	0.3802
10	1	3	13.8045	-335.0361	13.6878	0.4762	0.4519	0.3103
10	2	3	16.2418	-344.5794	14.8749	0.4062	0.3487	0.2379
10	3	3	16.8293	-346.0081	14.8349	0.4712	0.3312	0.3145
10	4	3	16.9641	-346.2954	14.2685	0.4753	0.3114	0.2069
10	5	3	13.4988	-333.6304	14.8388	0.3910	0.3436	0.4231
10	6	3	14.1614	-335.7151	14.6958	0.4021	0.3528	0.2450
10	7	3	16.3729	-344.5739	14.5501	0.4322	0.3589	0.3689
10	8	3	14.3925	-337.2337	15.3207	0.5258	0.4031	0.2355
10	9	3	15.5946	-341.7046	15.1710	0.3777	0.4358	0.2578
10	10	3	10.6622	-319.1220	14.2352	0.5328	0.3867	0.1413
10	11	3	13.6189	-334.2899	14.9800	0.4927	0.3524	0.3386
11	1	3	17.7998	-349.1187	16.0509	0.1915	0.3247	0.4160
11	2	3	14.7415	-338.2120	14.6721	0.4168	0.3615	0.3289
11	3	3	13.5504	-333.6424	14.3163	0.4266	0.3849	0.3872
11	4	3	17.5229	-347.9991	14.9030	0.3529	0.3440	0.2001
11	5	3	14.1669	-336.8316	14.8886	0.4595	0.4039	0.3552
11	6	3	15.8916	-342.8126	14.6115	0.3500	0.2910	0.4290
11	7	3	14.6642	-337.9523	15.9963	0.3798	0.4131	0.3541
11	8	3	15.0059	-339.5557	14.6481	0.4861	0.3300	0.2367
11	9	3	12.5989	-329.3052	14.0933	0.4037	0.4050	0.2901
11	10	3	15.1188	-339.5088	14.9177	0.5265	0.2581	0.2487
11	11	3	12.5237	-328.9834	15.3432	0.4805	0.3294	0.2265

RESULT OF MERGED CLASS

```
9  9  9  9  9  9  9  9  9  9  9
9  9  9  9  9  9  9  9  9  9  9
9  9  2  2  2  2  2  2  2  9  9
9  9  2  2  2  2  2  2  2  9  9
9  9  2  2  2  2  2  2  2  9  9
9  9  2  2  2  2  2  2  2  9  9
9  9  2  2  2  2  2  2  2  9  9
9  9  2  2  2  2  2  2  2  9  9
9  9  2  2  2  2  2  2  2  9  9
9  9  9  9  9  9  9  9  9  9  9
9  9  9  9  9  9  9  9  9  9  9
```

Appendix A. Sample output of initial calculation.

REFERENCES

1. R.L. Kashyap, P.M. Lapsa, "Synthesis and Estimation of Random Fields Using Long-Correlation Models", IEEE Trans. Pattern Analysis and Machine Intelligence, Vol. PAMI-6, No. 6, pp. 800-808, November 1984.

2. P. Whittle, "On Stationary Process in the Plane", Biometrika, Vol. 41, pp. 434-449, 1954.

3. W.E. Larimore, "Statistical Inference on Stationary Random Fields", Proc. IEEE, Vol. 65, No. 6, pp. 961-970, June 1977.

4. R.L. Kashyap, "Random Field Models on Finite Lattices for Finite Images", Proc. 5th International Conf. on Pattern Recognition, Miami, Florida, December 1980.

5. R. Chellapa, R.L. Kashyap, "Synthetic Generation and Estimation in Random Field Models of Images", Proc. Conf. PRIP, Dallas, Texas, pp. 577-582, 1981

6. R.L. Kashyap, R. Chellappa, "Estimation and Choice of Neighbors in Spatial Interaction Models of Images", IEEE Trans. Information Theory, Vol. IT-29, pp.60-72, January 1983.

7. R. Chellapa, R.L. Kashyap, "Texture Synthesis Using 2-D Noncausal Autoregressive Models", IEEE Trans. Acoustics Speech and Signal Processing, Vol. ASSP-33, No. 1, pp. 194-203, Februry 1985.

8. R.L. Kashyap, P.M. Lapsa, "Image Identification and Segmentation According to Random Field Models", Image and Vision Computingi, Vol. 1, No. 4, pp.189-195, November 1983.

9. R.L. Kashyap, "Optimal Choice of AR and MA Parts in Autoregressive Moving Average Models", IEEE Trans. Pattern Anal. and Machine Intell., Vol. PAMI-4, No. 2, pp. 99-104, March 1982.

10. R. Chellappa, R.L. Kashyap, "Statistical Inference in Gaussian Markov Random Field Models", Proc. Conf. PRIP, Las Vegas NV, pp. 77-80, June 1982.

11. A. Rosenfeld, L.S. Davis, "Image Segmentation and Image Models", Proc. IEEE, Vol .67, No. 5, pp.764-773, May 1979.

12. K.S. Fu, J.K. Mui, "A Survey on Image Segmentation", Pattern Recognition, Vol. 13, No. 1, pp.3-16, 1981.

13. C.W. Therrien, "An Estimation-Theoretic Approach to Terrain Image Segmentation", Computer Vision and Graphics and Image Processing, Vol. 22, pp.313-326, 1983.

14. J.E. Bevington, R.M. Mersereau, "A Maximum Likelihood Approach to Image Segmentation by Texture", Proc. Conf. ASSP, pp. 32.7.1-32.7.4, 1984.

15. S.L. Horowitz, T. Pavlidis, "Picture Segmentation by a Tree Traversal Algorithm", Jour. of ACM, Vol. 23, No. 2, pp. 368-388, April 1976.

16. P.C. Chen, T. Pavlidis, "Image Segmentation As An Estimation Problem", Comp. Vision and Graphics and Image processing, Vol. 12, pp. 153-172, 1980.

17. J. Besag, "Spatial Interaction and Statistical Analysis of Lattice Systems", Jour. of Royal Statistics Society B, Vol. 36, No. 2, pp. 192-236, 1974.

18. R.M. Bolle, D.B. Cooper, "Baysian Recognition of Local 3-D Shape", IEEE Trans. Pattern Anal Mach Intel, Vol. PAMI-6, No. 4, July 1984.

19. P. Brodatz, Textures - A Photographic Album for Artists and Designers, Dover, 1966.

20. D.L. Milgram, "Region Extraction Using Convergent Evidence", Comp. Graphics and Image Processing, Vol. 11, pp. 1-12, 1979.

21. A. Rosenfeld, "Problems, Progress and Prospects", Pattern Recognition, Vol. 17, No. 1, pp. 3-12, January 1984.

22. P.M. Lapsa, "Rough Notes on Model Choice", Personal Communication, 1984.

23. R.M. Haralick, GIPSY User's Manual, Volume 1, Spatial Data Analysis Laboratory, August 1983.

The vita has been removed from
the scanned document